Fall 12-1-2020

Validation of an Inertial-Measurement-Unit System for Calculating Hip and Knee Flexion Angles During Gait

Joonsun Park

VALIDATION OF AN INERTIAL-MEASUREMENT-UNIT SYSTEM FOR CALCULATING HIP AND KNEE FLEXION ANGLES DURING GAIT

by

Joonsun Park

A Thesis
Submitted to the Graduate School,
the College of Education and Human Sciences
and the School of Kinesiology and Nutrition
at The University of Southern Mississippi
in Partial Fulfillment of the Requirements
for the Degree of Master of Science

Approved by:

Dr. Nuno Miguel Moreira Cancela Oliveira, Committee Chair
Dr. Paul Donahue
Dr. Zhanxin Sha

December 2020

Published by the Graduate School

ABSTRACT

Technological advances regarding Inertial Measurements Units (IMUs) have positioned this type of sensor as an alternative for camera-based motion capture. This study introduces a new IMU based system (IMU_{sys}) to measure hip and knee flexion angles. PURPOSE: To validate the use of a five-sensor IMU_{sys} for the measurement of knee and hip flexion angles during gait in adults and pediatrics at two different time points. METHODS: Bilateral hip and knee flexion patterns (LH, RH, LK, and RK) of twenty-two healthy participants (12 adults and 10 pediatric) between the ages of 8 – 35 years were investigated. Participants performed two 1-min gait trials on a treadmill at self-selected speeds at two different time points. Data were analyzed using linear regression coefficients, the root mean square error (RMSE), the mean absolute error (MAE), and Bland & Altman plots. RESULTS: A strong relationship ($r^2 > 0.94$) between the IMU_{sys} and the camera-based system was found across all condition. RMSEs [LH < 10°, RH < 10°, LK > 10°, RK > 10°] were found across all condition. Repeatability coefficients [LH ≤ 5°, RH ≤ 5°, LK > 10°, RK < 10°] were found across all condition. CONCLUSION: The validity of the IMU_{sys} was maintained across age groups with different segment proportion, and during prolonged use. However, the large errors observed for knee flexion measurements should be considered when using the IMU_{sys}.

ACKNOWLEDGMENTS

I would like to record my gratitude to a number of individual who have given me help and encouragement over the period in which this thesis is written.

I wish to express my deepest gratitude to Dr. Nuno Oliveira who always helped me to advance to where I had to be throughout my thesis. He conveyed a spirit of adventure in regard to research and a lot of energy and enthusiasm in regard to teaching. Without his mentoring, this thesis would not have been possible.

I would like to express my special appreciation to Dr. Paul Donahue and Dr. Zhanxin Sha for sacrificing their time to give the advice and insightful comments in the writing of this thesis.

In addition, invaluable help was furnished by Dr. Matthew Jessee who gave me an opportunity to get on the right foot for my research journey in the United States.

Also, I extended my gratitude to Daphney Standford who gave me a tremendous help throughout her Master's degree.

TABLE OF CONTENTS

LIST OF TABLES

LIST OF ILLUSTRATIONS

LIST OF ABBREVIATIONS

ASIS	Anterior Superior Iliac Spine
CBMC	Camera Based Motion Capture System
DLT	Direct Linear Transformation
GCS	Global Coordinate System
HHM	Helen Hayes Model
IMU	Inertial Measurement Unit
IMU_{sys}	The tested Inertial Measurement Unit System
LCS	Local Coordinate System
LLA	Lower Limits of Agreements
MAE	Mean Absolute Error
Mdif	Mean of The Differences
PIG	Plug-in Gait
PSIS	Posterior Superior Iliac Spine
RMSE	Root Mean Square Error
RPC	Repeatability Coefficient
RPC_{np}	Non-parametric Repeatability Coefficient
ULA	Upper Limits of Agreement

CHAPTER I - INTRODUCTION

Camera-based motion capture systems (CBMCs) have been frequently used to assess whole-body kinematics. Due to their high accuracy, these systems have been established as the 'gold standard' in measuring anatomical movements, and have been commonly applied in research and clinical settings.

Despite their high accuracy, CBMCs have several limitations: 1) Time-consuming setups and calibration procedures (Sharma & Sharma, 2013). 2) Require a motion capture volume within the designated multiple camera zone and configuring reflective markers on participants (Cutti et al., 2010; Robert-Lachaine et al., 2017). 3) May require clinical populations to have to stand in anatomical positions during the calibration process. 4) Require technicians who have considerable expertise in dealing with different types of the systems, differences in biomechanical models, marker placements and configuration (Agustsson et al., 2019; Taylor et al., 2017). Finally, the systems are expensive and hardly portable thus have been confined to the laboratory setting. This environment may limit participants' strides per trial and prescribe their natural performance for data collection.

Over the last decade, technological advances have introduced alternative tools for studying human kinematics. Inertial Measurement Units (IMUs) are electronic devices with embedded sensors (Nymoen, 2014) that measure the orientation of a body. The units are small and light enough to be placed on body segments. The output of the units is integrated in a model, and anatomical angles can be calculated in reference to a calibration position (Cuesta-Vargas et al., 2010; Fong & Chan, 2010). Due to their portability and quick setup procedures, this type of system might be beneficial for testing

and studying clinical populations. However, the validity of the measurements provided by the IMU system should be established before its application and use. Typically, to determine the validity of IMU based joint angle measurements a CBMC is used as the 'gold standard'. A few studies have been devoted to the accuracy of IMU systems to calculate many joint motions (Cuesta-Vargas et al., 2010; Poitras et al., 2019). However, these studies investigated the validity of an IMU system that is expensive and uses a proprietary algorithm. Moreover, the effects of prolonged use of the system or differences in segment proportions, typical of different age groups, should be investigated.

The current study investigates the validity of a newly developed five-sensor IMU system (IMU_{sys}) to calculate bilateral hip and knee flexion angles during gait. Gait at self-preferred speeds in adults and adolescents at two different time points was investigated. The results of this study could help inform whether the IMU_{sys} can be a potential alternative to traditional CBMCs.

Hypotheses

The hypotheses for this study are as follow:

H_{01}: The root mean square error for hip joint angles will be less than 10 degrees.

H_{A1}: The root mean square error for hip joint angles will be greater than 10 degrees.

H_{02}: The root mean square error for knee joint angles will be less than 10 degrees.

H_{A2}: The root mean square error for knee joint angles will be greater than 10 degrees.

H_{03}: The repeatability coefficient for hip joint angles will be less than 10 degrees.

H_{A3}: The repeatability coefficient for hip joint angles will be greater than 10 degrees.

H_{04}: The repeatability coefficient for knee joint angles will be less than 10 degrees.

H_{A4}: The repeatability coefficient for knee joint angles will be greater than 10 degrees.

CHAPTER II - LITERATURE REVIEW

Inertial measurement unit based (IMU) systems have been widely used as an alternative tool that can complement the shortcomings of camera based motion capture systems (CBMCs). Recent years have witnessed the validation of IMU systems to calculate specific joint motions. However, to author's knowledge, no definitive answer has been given to the question of the validation of IMU systems in both pediatrics and adults. Also, no studies have been done for the validation of IMU systems during prolonged use. Thus, the purpose of this study was to determine the accuracy of a five-sensor inertial measurement unit system for calculating bilateral hip and knee flexion angles during gait at self-selected speeds in pediatrics and adults at two different time points.

2.1. Camera-Based Motion Capture Systems

CBMCs are commonly used to analyze movements in the three dimensional space (Fernández-Baena et al., 2012). CBMCs use infrared video cameras to track retro-reflective markers, or reflective markers, attached to the skin to reconstruct the movement into three dimensional coordinates (Bodenheimer et al., 1997; Sharma & Sharma, 2013). This type of technique has been widely applied to many different fields such as gaming, filmmaking, and biomechanical analysis of movement (Aurand et al., 2017; Cappozzo et al., 1995; Sharma & Sharma, 2013; Zhang et al., 2013).

2.1.1. CBMCs Methodology

Capturing the movements of an object with the cameras means that each camera records the movements of retro-reflective markers attached to the object. A marker is a small finger-sized sphere, and marker sets are affixed to an object or a body segment of interest to help the cameras measure the locations and orientations of the body segments. There are two types of markers: active markers and passive markers. Active markers are to illuminate light by itself. Passive markers are to reflect light through the surrounding light (Allard et al., 1995).

The physical space and environment during data collection should be considered when using CBMCs. A controlled room is required to capture kinematic human movements to minimize errors (Fernández-Baena et al., 2012). The term ‘kinematic’ refers as the description of motion of an object. The controlled room can refer to an environment that is set up to capture the markers fixated on a kinematic human model without any obstructions. Anything that can be reflective or brighter than markers have to be avoided out of the field of view of the camera. Field of view is defined as the single rectangular area (or plane) seen by a camera’s optics. The light sources should spread and adjust evenly. These conditions play a role in optimizing that optical cameras only recognizes the markers set by the observers (Nymoen, 2014).

In addition, the number of cameras and the position of cameras should be considered in order to represent a kinematic human model in real time into a three dimensional image. At least two cameras are required and the direction of the cameras must be toward the space within which the markers’ movement falls.

To quantitatively collect kinematic data, CBMCs are required to construct a fixed global coordinate system (GCS) (Robertson et al., 2013). The GCS refers to the measured capture volume that represents the three dimensional space (Robertson et al., 2013).

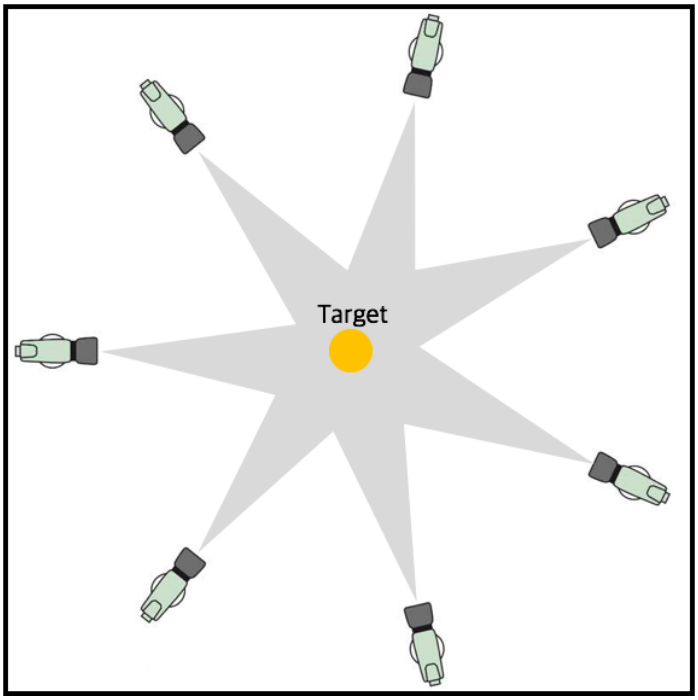

Figure 2.1. *Typical controlled camera based motion capture room with multi-cameras set up for analyzing human motion. The cameras' fields of view overlap in the global coordinate system.*

To define the GCS, the center of the space is calibrated with a static calibration object ('L frame') and a dynamic calibration object ('T frame') that includes a series of the reflective markers (Iwan, 2006; Nymoen, 2014). The 'L frame' determines what directions of the coordinate axes will be. This static calibration object is positioned on the floor in the center of the space to be calibrated where the cameras' fields of view overlap. Each camera records the 'T frame' markers displacement so that this dynamic calibration object helps the static calibration object define the directions of the coordinates axes

within a predetermined capture volume. The trajectories transmitted by each camera's view are recorded in two-dimensional coordinates. In order to extract tangible three-dimensional data with real metric units, direct linear transformation (DLT) method is applied (Abdel-Aziz & Karara, 2015). This method transforms the two-dimensional digitized coordinates to real three-dimensional metric units (i.e. X, Y, and Z).

To provide the locations and orientations of a body segment or a rigid body in relations to the GCS, a moving local or segment coordinate system (LCS) needs to be established on the body segments of interest (Nymoen, 2014; Robertson et al., 2013). The LCS is defined by each marker placed on the body segments of interest with respect to the GSC. Axes of LCS are roughly aligned with axes of GCS in the same directions when a human kinematic model poses in the anatomical position. When the body segments are moving along with the markers, the location and orientation of the LCS are recorded within the GCS and the axes of the LCSs are translated and rotated in space correspondingly (Robertson et al., 2013).

2.1.2. Anatomical Frames of Reference

In order to define the LCS in the anatomical segments of interest, several biomechanical models for three-dimensional gait analysis have been used (Baker et al., 2017; Kirtley, 2006; Vicon Motion Systems Limited, 2016).

2.1.3. Plug in Gait Model

Vicon developed the Plug-in gait (PIG) model (Figs. 2.2. - 2.4.), supported by individuals who contributed to the past models of movement analysis systems (Baker et

al., 2017). For the pelvis, four markers are required. A marker is located over the right and left anterior superior iliac spine (ASIS). The other two markers are placed over each right and left posterior superior iliac spine (PSIS). To estimate the right and left hip joint centers, the PIG model uses the Davis regression equations which automatically creates the hip joint centers (Davis et al., 1991), where the greater trochanters of femur are represented as bony hip joint landmarks (Kirtley, 2006). The markers are not needed for these landmarks. For the knee joint landmark, the markers are placed to the lateral sides of femur epicondyle to define the axis of the rotation of the knee passing through here. The marker should be lay in line with the estimated hip joint center. The right and left thigh markers are placed along the midline from its greater trochanter and the knee joint on both sides of femur. Both markers should not be horizontally laid on the same straight line but should be placed below the swing of the hands to prevent the markers from being knocked off (Vicon Motion Systems Limited, 2016). For example, one marker can be attached over the distal 1/3 of thigh, and the other marker can be attached over the proximal 1/3 of thigh. Both sides of shank marker placement are along the midline from the knee joint landmark and lateral malleolus that defines the ankle joint center. The shank markers should not be placed at the same height in the length of tibia. The way of shank marker placement can be applied in the same way of the thigh marker placement. For the foot, a marker is attached on the calcaneus heel and over the second metatarsal head.

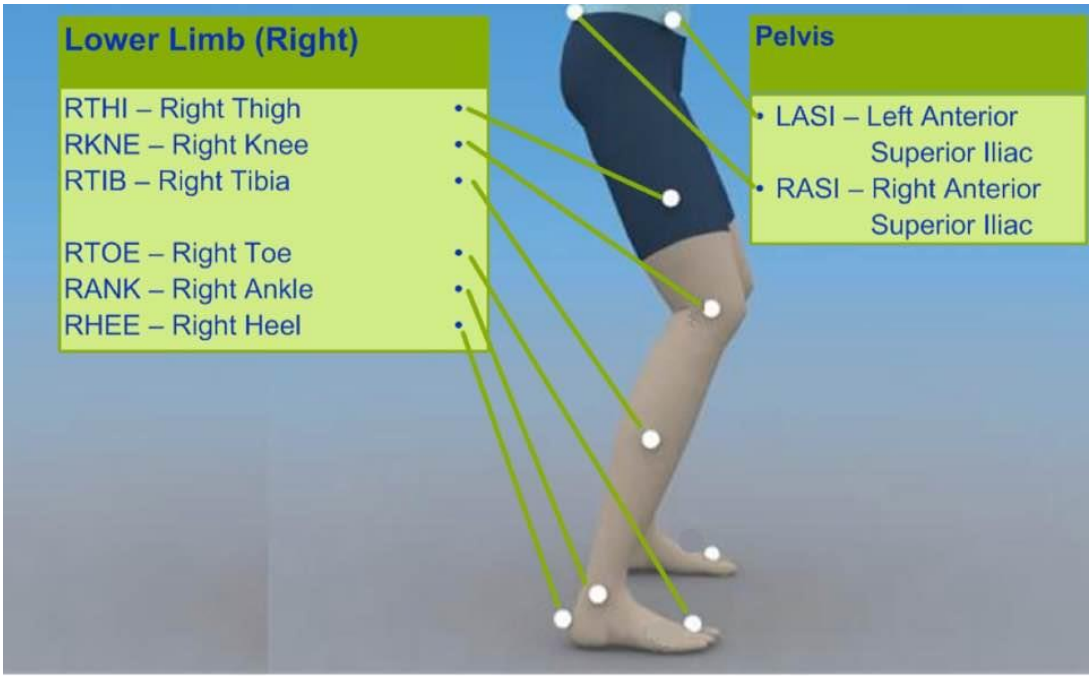

Figure 2.2. *Marker placement of lower body for Plug-in Gait model in the lateral view.*

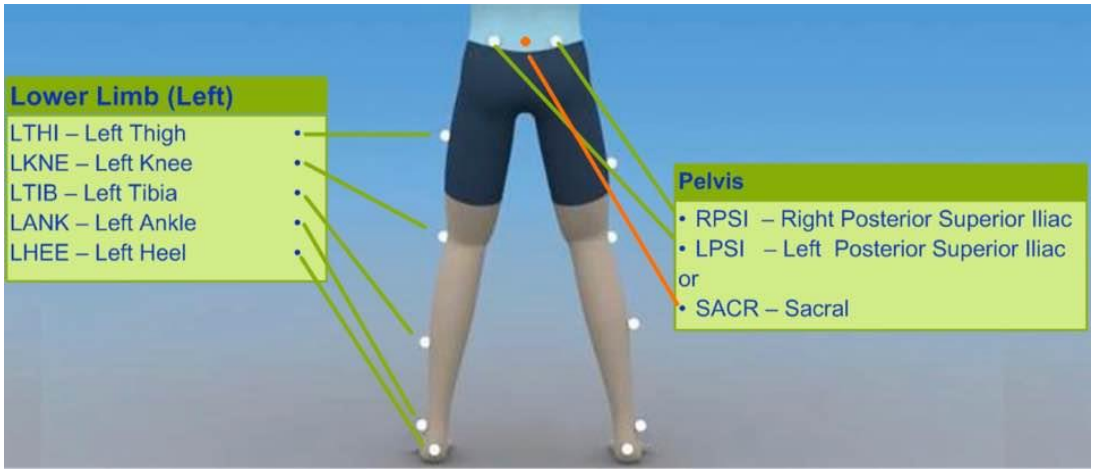

Figure 2.3. *Marker placement of lower body for Plug-in Gait model in the posterior view.*

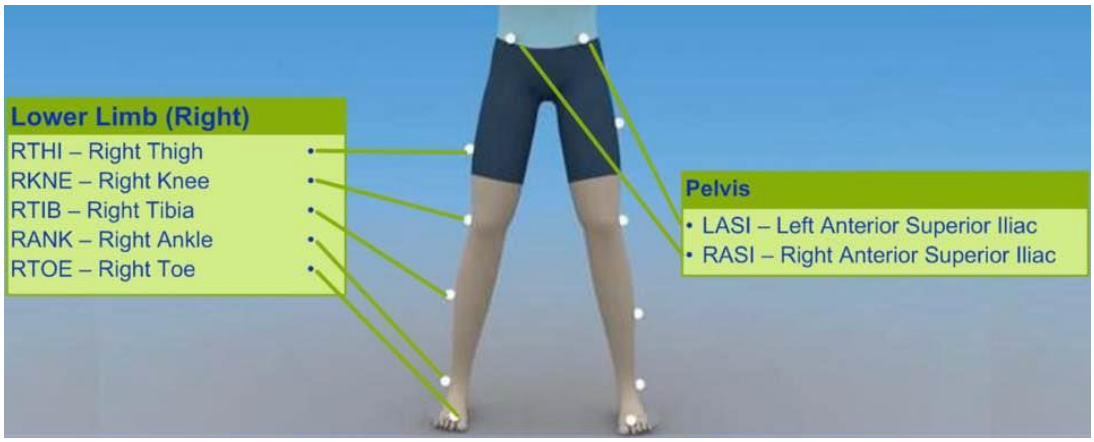

Figure 2.4. *Marker placement of lower body for Plug-in Gait model in the frontal view.*

2.1.4. Helen Hayes Model

There are various names for Helen Hayes Model (HHM): Modified Helen Hayes, Vaughan, Newington, Kadaba, Davis, Gage, or Vicon Clinical Manger model (Kirtley, 2006). For the pelvis, HHM starts with three markers on the right and left ASIS and the spinous process of the second sacral vertebra (S2) which is located on the midpoint of the right and left PSIS. HHM uses Davis regressions equations described by Bell et al. (1990) and Davis et al. (1991) for defining the location of the hip joint center. The other marker placements for thigh, knee, shank, ankle and foot are the same as the placements that the markers are attached over the thigh landmark, the knee joint landmark, ankle joint landmark and the foot land marker in the PIG model. However, a marker on the thigh is placed on the Velcro strap with a short stick, or wand to form a triangle defining the thigh. The Velcro strap is wrapped over the thigh, and the wand with a marker placed is fixed on the strap. The height of the strap' location is not critical, but it should be placed out of swing of a hand. A marker for the shank is straightforward. The shank landmark is

indicated by a wand with a marker but the position of a marker for shank is similar to the position of the maker used in the PIG model.

Figure 2.5. *Marker placement of lower body for Helen Hayes model in the frontal and posterior views.*

2.1.5. Cleveland Clinic Model

The Cleveland Clinic model, implemented in the Orthotrack software by Motion Analysis Corporation, used to commonly be used in the past (Baker et al., 2017). However, due to a lack of literature on validation of the Cleveland Clinic model, it has not widely been used (Baker et al., 2017). The Cleveland Clinic model uses the same placement for three pelvis markers as the HHM uses for the pelvis. The Cleveland Clinic model uses a cluster of markers, which consists of a set of at least three noncollinear markers attached on a strap. A cluster of makers is strapped around the thigh and the

shank. Compared to a wand with a marker, an advantage of a marker cluster or triad is to be less sensitive to placement errors while the body segments are in motion.

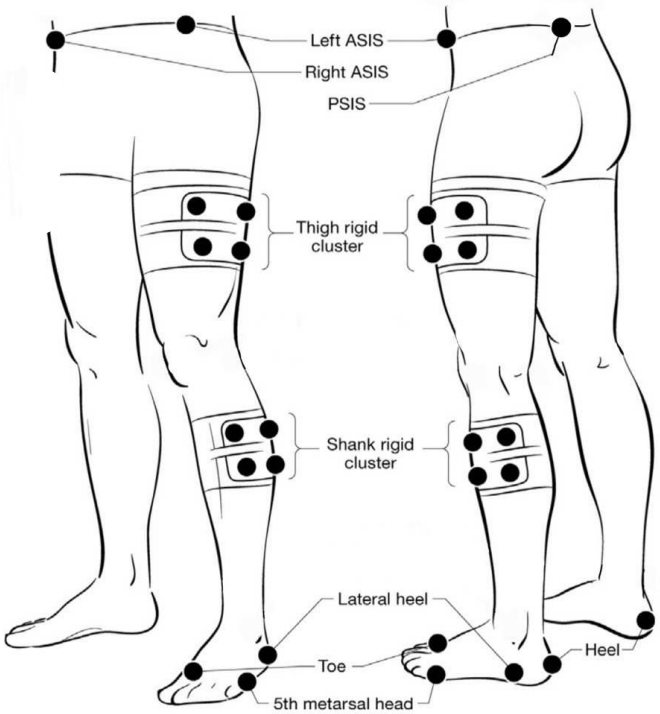

Figure 2.6. *Marker placement of lower body for Cleveland Clinic model in the frontal and posterior views.*

2.1.6. Limitations of CBMCs

Three-dimensional techniques for motion capture should be used by researchers whenever the objective is the accurate and detailed investigation of movements that occur in several planes. However, CBMCs also present several limitations (Robertson et al., 2013; Yordanova et al., 2016):

- Have time-consuming setup and calibration procedures (Sharma & Sharma, 2013; Yordanova et al., 2016). In fact, it takes a considerable amount of time not only to set up the controlled space and multiple cameras to be properly positioned, but also

to construct the GCS with a static calibration wand and a dynamic calibration wand followed by the LCS with IMUs for calibration.

- A motion capture volume within the designated multiple camera zone and configuring reflective markers on participants is required.
- The process may require clinical populations to have to stand in anatomical positions during the calibration process.
- Require technicians who have considerable expertise in dealing with different types of the systems, knowing differences in biomechanical models and marker's configuration (Agustsson et al., 2019; Taylor et al., 2017).
- Are expensive.
- Hardly portable thus have been confined to laboratory settings or a specific area (Cutti et al., 2010; Robert-Lachaine et al., 2017).
- Although laboratory settings enables cameras to easily avoid reflective objects between the markers on participants' limbs, it may limit participants' strides per trial and prescribe their natural performance for data collection by influencing their psychological conditions, which may be dissatisfying in terms of meaningful biomechanical information (Cutti et al., 2010).

2.2. Inertial Measurement Unit based Systems

IMUs have been recently introduced as alternatives to CBMCs (Fong & Chan, 2010; Fusca et al., 2018; Mancini et al., 2016; McGinnis, 2013; Poitras et al., 2019; Zhang et al., 2013). An IMU is an electronic device that measures kinematic movements and provides data by using accelerometers, gyroscopes, and magnetometers (Cuesta-

Vargas et al., 2010; Fong & Chan, 2010; Poitras et al., 2019). Accelerometers measure linear acceleration providing a static orientation in X, Y, and Z axis continually being affected by gravity ($9.8m/s^2$). Gyroscopes measure angular velocity relative to X, Y, and Z axes (i.e. pitch, yaw, and roll). Magnetometers locate sensors orientation relative to Earth's magnetic field. Also, magnetometers, by estimating magnetic field intensity around in X, Y, and Z planes, helps to compute the orientation calculated from the accelerometers.

IMUs measure the orientation of a body relative to a global frame of reference (i.e. an initial references or starting position). Therefore, the angular movement of a joint linked by two segments, with an IMU each, can be calculated (Fong & Chan, 2010; Nymoen, 2014; Poitras et al., 2019).

2.2.1. Application of IMUs in Gait Analysis

Zhang et al. (2013) examined the validity of an IMU based system (Xsens MVN BIOMECH; Xsens Technologies BV, Enschede, The Netherlands) compared to a CBMC (NDI Optotrack 3020 system; Northern Digital Inc., Ontario, Canada). They found that there was a similar waveform between two systems in a gait cycle for the knee and the hip sagittal plane (extension/flexion) during an over-ground walking test. However, they concluded that caution should be exercised when the kinematic outputs in the frontal plane (adduction/abduction) and the transverse plane (internal/external) from two systems are compared. They explained that the existence of the offset is mainly caused by the determination of the actual joint center from different anatomical reference frames which are concerned as a major contributor to the discrepancy. They followed the proprietary

sensor configuration that Xsens MVN BIOMECH suggests. For the CBMC (NDI Optotrack), the marker configuration are followed by the International Society of Biomechanics.

Al-Amri et al. (2018) reported the finding in hip and ankle joints from two systems must not be interpreted interchangeably due to two different types of the anatomical frame used. In this study, they examined the validity of the same IMU system that Zhang et al. (2013) used, comparing to VICON motion analysis system. The marker placements of the CBMC were provided based on the PIG model (Vicon Motion Systems, Oxford Metrics Group Ltd.), and the sensor's configuration was followed by the Xsens manual (Xsens Technologies). The kinematic data between two systems appeared to have similarity in the knee and hip angles in all three planes. They found that there was excellent similarity in the waveform pattern for the sagittal plane knee angle and the sagittal plane hip angle between two systems in a walking condition. In addition, an excellent similarity was found in the waveform pattern for the frontal plane hip angle in the same walking condition. There was a moderate similarity in the waveform pattern for the transverse plane angle and the frontal plane knee angle in the same walking condition as well. However, they pointed out that the discrepancy in the waveforms caused by two different biomechanical model did not narrow enough.

In contrast, Bessone et al. (2019) drew a relatively positive conclusion in that the aktos-t system (myolution GmbH, Ratingen, Germany) provided acceptable measurements for the hip and knee angles. However, they drew the conclusion only with respect to the sagittal plane. In the waveforms of a gait cycle for the hip and knee, they found significant difference at 50 – 70% of the gait cycle for the hip and knee in the

sagittal plane, which corresponds to the phase from the end of the pre-swing phase to the beginning part of the mid swing phase. Bessone et al. (2019) indicated the major cause of the differences between two systems was the PIG model (Vicon Motion Systems) that the CBMC (Vicon Motion Systems, Oxford, UK) employed. They stated the PIG model created errors during wide ROMs (Besier et al., 2003) in that the PIG model uses an anatomical joint center, not a function joint center.

2.2.2. Limitations in the use of IMU based systems

There are a limited amount of studies investigating the validity and the reliability of measurements from available IMU systems during clinically relevant functional activities (Al-Amri et al., 2018; Cutti et al., 2010; Ferrari et al., 2010; Picerno et al., 2008; Robert-Lachaine et al., 2017; Washabaugh et al., 2017; Zhang et al., 2013). These studies tended to show that correlation values are high for hip and knee with and without the removable offset (Al-Amri et al., 2018; Cutti et al., 2010; Ferrari et al., 2010; Picerno et al., 2008; Robert-Lachaine et al., 2017; Washabaugh et al., 2017; Zhang et al., 2013). However, the effect of segment anthropometry, typical of different age groups, or the duration of measurements has not been investigated. Examination of changes in accuracy for IMU based systems during long interventions may be warranted, as there is the potential for changes in the stability of IMUs.

2.3. Gait

Human gait refers to the way a person walks. The natural pattern of walking is that two multisegmented lower limbs intersect each other repetitively with

simultaneously maintaining stance stability to move the body forward (Kharb et al., 2011; Perry & Burnfield, 2010). When a leg goes forward, it is defined as a step. For example, when the right leg moves forward with the floor contact, this phase between the left leg and the right leg is a right step. Subsequently, when the left leg swings forward with the floor contact, it makes a left step. When two consecutive floor contacts occur with either of the same (right or left) lower limbs, it is called a stride in which there are two steps. The stride is the equivalent of a gait cycle. For example, a gait cycle occurs until a person takes an initial heel strike with the right leg then makes the subsequent heel strike with the right leg after the left leg (ipsilateral leg) swings.

2.3.1. Gait Cycle and its Phases

The beginning of the gait cycle is often determined by the initial contact, often called heel contact, or heel strike, of a foot. The end of the gait cycle is determined by the subsequent heel contact of the same foot, which will be the initial contact for the next gait cycle. A gait cycle falls into two periods, stance and swing. The stance period lasts approximately 60% of the gait cycle, from the point of heel strike to the point of toe-off (when the foot is off the ground). The swing period is approximately 40% of the gait cycle, from the point of toe-off to the point of the subsequent heel strike (Kirtley, 2006; Perry & Burnfield, 2010).The stance period begins with the initial heel contact of a foot and ends the toe-off of that foot. The swing period begins with its toe-off and ends at the second heel contact.

Double support, or double stance (Kirtley, 2006; Perry & Burnfield, 2010) is the state of both feet on the ground. The double support is divided into two periods, initial

double limb stance and terminal double limb stance. In the initial double limb stance, body weight is transferred to a foot that makes heel strike from contralateral foot. In the terminal double limb stance, body weight is transferred to contralateral foot from ipsilateral foot that makes toe-off (Kharb et al., 2011).

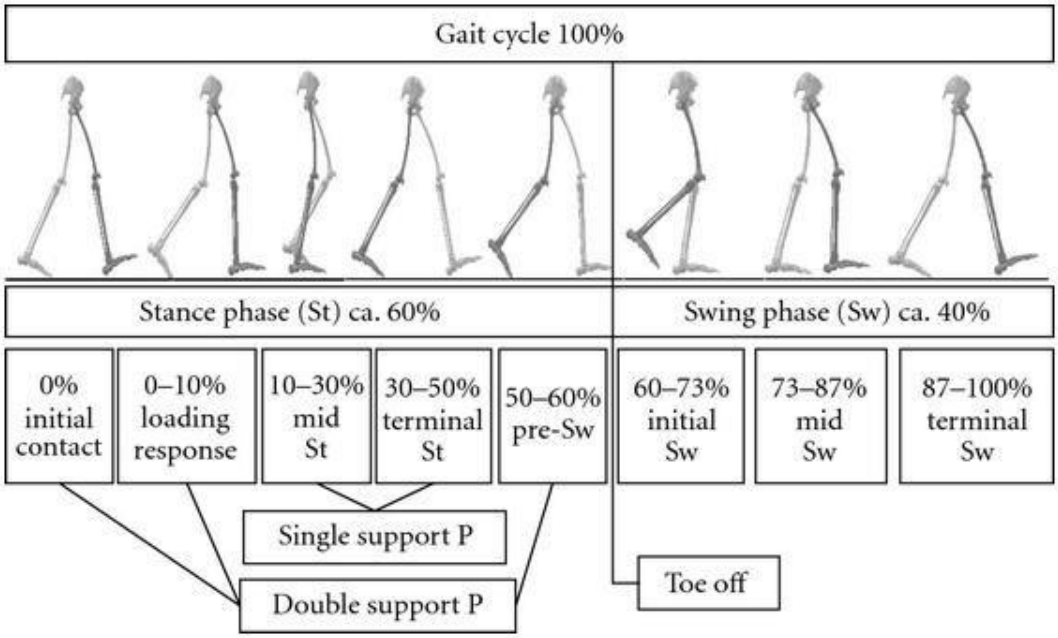

Figure 2.7. *Illustration of the events of the gait cycle*

Occasionally, these two stance periods can be termed single limb stance because with respect to center of mass, when contralateral foot is lifted from the floor, only one leg is supported on the ground. Kirtley (2006) pointed out that the double limb stance period can be an major indicator of walking because as the speed of walking increases, the two double stance periods in a gait cycle gets shorter. Eventually, no double support periods exist during running.

Walking is performed mostly by three multisegmented lower limbs such as the hip, knee, and ankle to move the body forward. It is challenging to have well-satisfied comprehension of the lower limbs' articulations in a gait cycle. Perry & Burnfield (2010) addressed a series of a person's walking patterns by categorizing a gait cycle based on three basic tasks, which are weight acceptance, single limb support, and limb advancement. The three tasks are subdivided into eigth phases based on functional characteristics of individual joint motion occurring. The eight phases are involved: initial contact, loading response, mid stance, terminal stance, pre swing, initial swing, mid swing, terminal swing. Thus, it is imperative to explore how structurally multisegmented lower limbs that occur simultaneously are coordinated in accomplishing three tasks through each phases. Also, this approach can aid to comprehend and interpret all the curves in the graphs indicating individual joints motion in a gait cycle because the curves summarizing joint kinematics regarding a gait pattern can be bewildering to analyze.

2.3.2. Hip Flexion

In initial contact phase (0 – 2 %), the hip is flexed when initial floor contact is made with the heel of the foot moving forward. In loading response phase (0 – 10%), the body weight is transferred onto ipsilateral limb from contralateral foot that is at the end of terminal stance followed by having the hip begin extended. Therefore, it can be said that the weight acceptance task is accomplished in the initial double stance period.

The single limb support task is accomplished by mid stance and terminal stance phases. Mid stance phase (10 – 30%) begins with lifted-contralateral toe and ends the body weight is loaded over ipsilateral limb (Gage, 1990). The hip is extended with ankle

dorsiflexed, causing the body to advance in the first half of ipsilateral limb support. Terminal stance phase (30 – 50%) begins when the body weight is over ipsilateral limb and ends when the floor contact is made with contralateral heel (Gage, 1990). The hip creates more flexion, and the heel of ipsilateral limb rises from the ground as the center of mass continues advancing in front of the hip and ipsilateral limb. The limb advancement task is accomplished by pre-swing, initial swing, mid swing, and terminal swing phases. Pre-swing phase (50 – 60%) begins with loss of hip extension on ipsilateral leg and ends with hip flexion being initiated (Gage, 1990). In this phase, ipsilateral thigh moves forward as hip flexion is increased with increased ankle plantar flexion. Initial swing phase (60-73%) begins with ipsilateral hip flexion (swinging limb) and ends until ipsilateral knee maintains flexion to neutral (Gage, 1990). In this phase, the hip flexion is induced to begin advancement of the body forward with the ankle partially dorsiflexed. In mid swing phase (73 – 87%), the hip flexion of the swinging limb continues. It continues moving forward until the tibia of the swinging limb is perpendicular to the ground (Gage, 1990). In this phase, the hip continues passively flexed until the thigh reaches its peak advancement. Cessation of hip flexion occurs in terminal swing phase (87 – 100%) in which is the final phase of the gait cycle for initial contact to begin the next gait cycle (Gage, 1990). The hip flexion of the advancing swing limb is completed maintaining its earlier flexion.

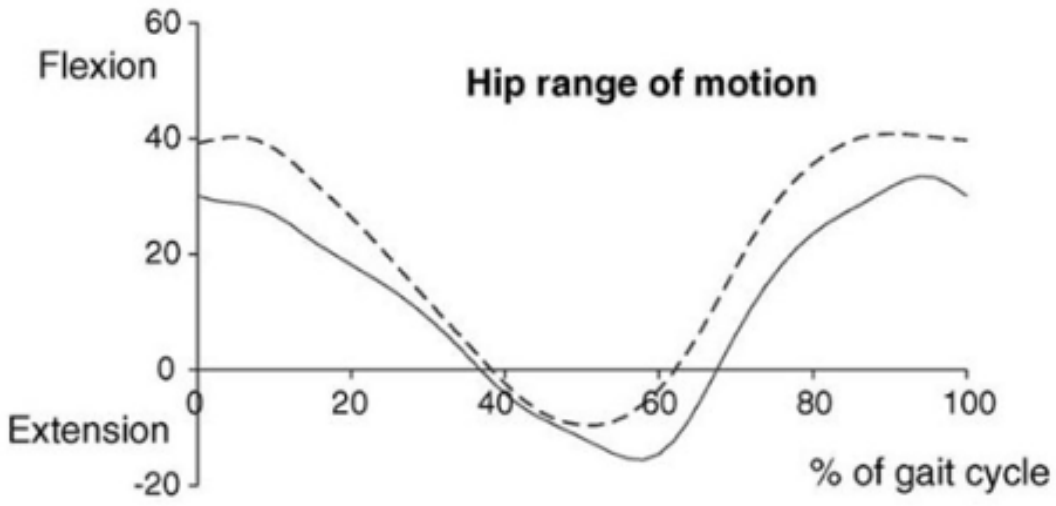

Figure 2.8. *The sagittal range of motion of the typical hip flexion and extension.*

2.3.3. Knee Flexion

In initial contact phase (0 – 2 %) of the weight acceptance task, the knee of the limb moving forward is fully extended as the heel of the limb strikes the ground. In loading response phase (0 – 10%), the knee flexes slightly because of shock absorption caused by the heel strike as the body weight is transferred onto the limb stroke the ground.

In mid stance phase (10 – 30%) of the single limb support task, while the knee extends, the body is advancing with the ankle dorsiflexed in the first half of the single limb support. In terminal stance phase (30 – 35%) of the single limb support task, the knee extension maintains followed by the slight knee flexion.

In pre-swing phase (50 – 60%) of the limb advancement task, the knee is greater flexed as ipsilateral limb is pushed and begin lifted off the ground. In initial swing phase (60-73%) of the limb advancement task, the knee reaches maximum flexion of a gait

cycle while ipsilateral limb is over the ground and is moving forward. In mid swing phase (73 – 87%) of the limb advancement task, as the ipsilateral thigh moves forward and reaches its peak advancement, the knee slightly extends until the tibia is vertical to the ground with the ankle naturally dorsiflexed. In terminal swing phase (87 – 100%) of the limb advancement task, greater knee extension occurs and complete ipsilateral limb advancement, aiding the heel to be positioned for initial contact to the ground. The ankle maintains dorsiflexion to neutral.

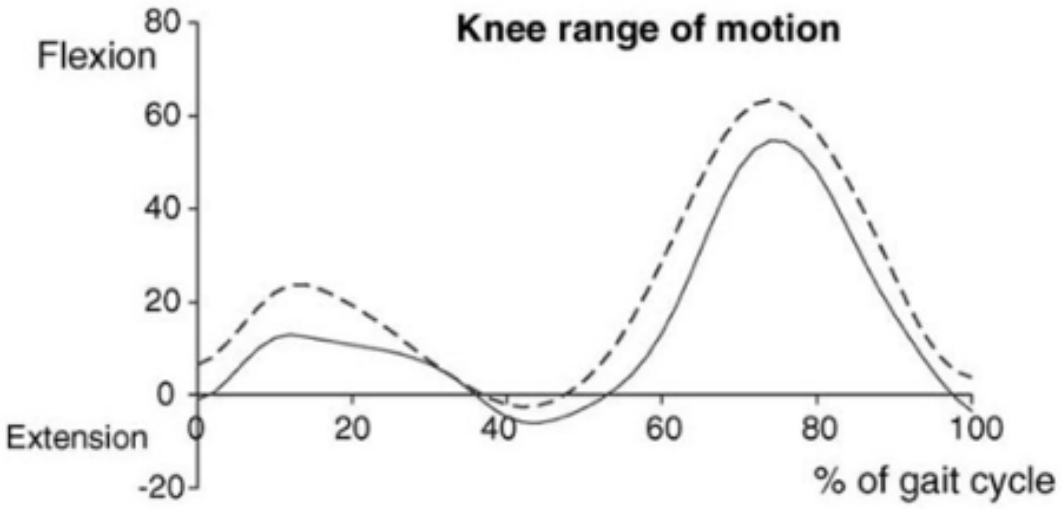

Figure 2.9. *The sagittal range of motion of the typical knee flexion and extension.*

2.3.4. Differences in gait features between pediatrics and adults

The analysis of age dependent gait patterns has been carried out since the 1980's (Smith et al., 2016). However, relatively little attention has been directed to differences in gait patterns or features between healthy pediatrics and adults. The gait study dedicated to develop a normal pediatric reference (5 ~ 16 years) reported the range of motion (ROM)

for the hip and knee (Ounpuu et al., 1991). When compared to the hip (flexion: 30°, extension: 10°) and knee (flexion: 65°, extension: 2°) in adults (Perry & Burnfield, 2010), the similar ROM for the knee and hip was found (Table 2.1).

Table 2.1. *Pediatrics' joint kinematic data.*

JOINT	FLEXION	EXTENSION
HIP	39°±7	16°±5
KNEE	65°±7	4°±6

(Ounpuu et al., 1991)

Table 2.2. *Pediatrics' joint kinematic data across age groups*

MOVEMENT		7 yrs.	8 yrs.	9 yrs.	10 yrs.	11 yrs.
HIP	**Flexion**	27.7°±5.2	28.4°±3.7	24.1°±6.4	29.2°±4.6	26.5°±4.5
	Extension	-7.7°±6.8	-8.7°±5	:-6.9°± 3.6	-8°±3.4	-7.5°± 3.8
KNEE	**Flexion**	47.9°±11.7	51.3°±8.5	39.9°±21.8*	45.7°±10.5	55.6°±3.1
	Extension	3°±6.8	-1.76°±3.7	-4.6°±7.7	3.6°±5.4	1.9°±5.4

*: Significant differences ($p<0.05$)

(Ciğali et al., 2011)

In a study by Ciğali et al. (2011) that examined the ROM for the hip and knee across age (Table 2.2), there was no significant difference in the ROM for the hip and knee across age groups except for the ROM for the knee flexion in the 9 years old group, suggesting 7 ~ 11 year-old children had similar gait pattern for the hip and knee to the adults had. In particularly, they found that there were two periods of knee flexion in pediatrics - the first flexion occurred during loading response, and the other flexion occurred during initial swing period, which was the same pattern seen in the adults' gait.

Although there was similar tendency in the joint kinematics across ages (5 ~ 16 years), the influence of physical changes on time-distance gait parameters (i.e. step frequency, step length, and walking velocity) should not be ignored (Aloba et al., 2019; Beck et al., 1981; Grieve & Gear, 1966; Norlin et al., 1981; Smith et al., 2016;

Sutherland, 1997; Wheelwright et al., 1993). Pediatrics around the age of 12 start puberty and go through rapid physical changes (Ferrari et al., 2008). It implied that change in gait features (i.e. step frequency, step length, and walking velocity) can be highly related to muscular-skeletal growth (Todd et al., 1989). Namely, the same or similar to adult's gait features will not be seen until muscular skeletal growth is fully completed.

CHAPTER III - METHODOLOGY

3.1. Participants

Ten typically developing pediatric individuals (8–17 years of age) and twelve healthy adults participated in this study (Table 3.1). Inclusion criteria included being able to understand written and spoken English and walk on a treadmill with any difficulties. Participants were excluded if they had significant orthopedic or neurological impairment that interfered with the ability to walk and significant recent surgery. The participants were recruited by email, classroom announcements, and word of mouth. All subjects provided written consent to participate. For the pediatric participants, informed consent was also obtained from a parent or guardian. All research procedures were approved by The University of Southern Mississippi Institutional Review Board.

Table 3.1. *Descriptive characteristics of both adults and adolescents.*

	Adults	**Adolescents**
Participants (N)	12; 6M, 6F	12; 8M, 4F
Age (years)	26.3 ± 5.9	13.6 ± 2.3
Height (cm)	173.7 ± 7.4	163.9 ± 14.1
Weight (kg)	74.8 ± 11.2	47.1 ± 11.9
Gait Speed (m/s)	0.82 ± 0.12	0.79 ± 0.17
Leg Length (cm)	81.5 ± 4.1	74.9 ± 7.0
Knee Width (cm)	10.68 ± 0.82	9.57 ± 1.2
Ankle Width (cm)	6.85 ± 0.3	6.51 ± 0.65

3.2. Participant Setup

Sixteen passive retro-reflective markers and five MTw motion sensors (Xsens MTw, Enschede, The Netherlands) were attached to the participant. The retro-reflective markers were placed bilaterally at the anterior superior iliac spine (ASIS), posterior superior iliac spine (PSIS), thigh, knee joint, shank segment, ankle, heel and toe according to the Plug-in Gait (PIG) model (Figs. 2.2. - 2.4.). To be specific, for the pelvis, a marker was attached over the bilateral ASIS and PSIS. For the knee joint, a marker was attached to the lateral side of the femur epicondyle. The marker was lay in line with the estimated hip joint center. For the thigh, a marker was attached along the midline from the femur greater trochanter to the marker on the knee joint. The other maker was attached on the other side of the thigh. However, the markers were not horizontally laid on the same level but below the swing of the hands to prevent the markers from being knocked off (Vicon Motion Systems Limited, 2016). For the shank, a marker was attached along the midline from the marker on the knee joint to the lateral malleolus that defines the ankle joint center. The other maker was attached on the other side of the shank. The shank markers was not attached at the same height in the length of tibia. For the foot, a marker was attached on the calcaneus heel and over the second metatarsal head.

Based on our custom developed IMU model, an MTw motion sensor was placed at the sacrum, and two MTw motion sensors were placed bilaterally at the thigh and shank. The thigh MTw motion sensor was placed on the anterior portion of the upper leg at half the distance from the anterior superior iliac spine to the superior part of the patella. The shank MTw motion sensor was placed along the midline of the posterior portion of

the lower leg at half the distance of tibia. The sensor alignment was horizontally exercised to minimize errors in hip and knee joint angles when an MTw motion sensor was attached on the bilateral segments.

Both retro-reflective markers and MTw motion sensors were securely attached using a double-sided adhesive tape. The MTw motion sensors at thigh and shank segments were wrapped in elastic plastic wrap one more time then secured in place using athletic tape to prevent a sensor from detaching from an original place.

Figure 3.1. *The placement of the IMU sensors and the retro reflective markers*

3.3. Experimental Protocol

Only one visit for the test was required for the study. The visit lasted approximately 120 minutes. Before the test, participants completed a History & Physical Questionnaire, and the Waterloo Footedness Questionnaires (van Melick et al., 2017).

Before the test, participants were asked to stand still in a static standing posture on a treadmill for 10 seconds for conducting the calibration of the retro-reflective markers and MTw motion sensors. Familiarization to walking on the treadmill then commenced while determining the preferred self-selected speed for the participant. Once a preferred self-selected speed was determined, participants were asked to walk at preferred self-selected speed for 1 minute on the treadmill before and after a treadmill walking protocol designed for a different experiment. The duration of the walking protocol was 37 minutes and included 28 minutes of walking and 9 minutes of rest (Fig. 3.1). For each 1-minute walking test, 20 seconds of steady state gait (the second 20 seconds of the test) were analyzed.

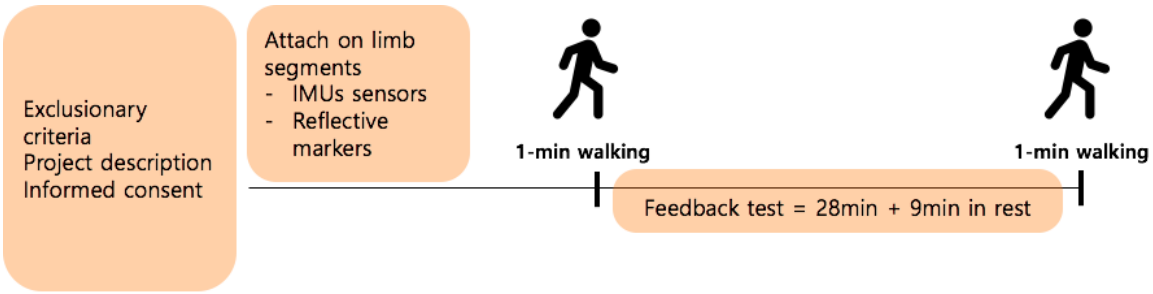

Figure 3.2. *The experimental design*

3.4. Data Processing

The IMU_{sys} hip and knee flexion angles were calculated as the difference between the sacrum-thigh and thigh-shank sensors' rotation about the sensor's longitudinal axis ('roll axis') respectively. A sampling rate of 60 Hz was used for both MTw motion sensors and CBMC (Qualisys, Göteborg, Sweden). The kinematic data from eight participants was initially collected at 100 Hz using the Qualisys system. For those participants, data was resampled to 60 Hz using the 'resample' function in Matlab (R2020a; The MathWorks Inc., Natick, MA, USA). Any missing frames in the three-dimensional trajectories were filled using a 3rd polynomial function that interpolates the data between the two points on both sides of the gap (Nymoen, 2014; Sharma & Sharma, 2013).

The cross-correlation function in Matlab ('xcorr') was used to align the signals in time by the optimization of a variable time offset. This process resulted in eight sets of 1200 paired samples of data for each participants (joint x side x time). All data were processed and synchronized with Matlab (Matlab R2019b, The MathWorks, USA).

3.5. Data Analysis

A linear regression was used to determine the linear strength of relationship between the IMU_{sys} and Qualisys. The coefficient of determination (r^2) indicated how much variance is shared between the IMU_{sys} and the Qualisys. The coefficients *m* ('slope') and *b* ('intercept') were calculated to describe the relationship between IMU_{sys} and Qualisys. The mean absolute error (MAE) and the root mean square error (RMSE)

were calculated to determine the average model prediction error in degrees. Bland & Altman 95 percentage limits of agreement (Martin Bland & Altman, 1986) was used to determine the agreement between the measurements from the IMU_{sys} and the Qualisys, and to visualize systematic errors between the IMU_{sys} and Qualisys.

The Kolmogorov Smirnov test was used to test for normality of the distribution of the differences between the IMU_{sys} and Qualisys. If the null hypothesis was rejected, a normal distribution was assumed. Therefore, the mean of the differences (Mdif) or 'bias' was calculated as the mean of the differences between IMU_{sys} and Qualisys measurements across all observations. The repeatability coefficient (RPC) was calculated as:

$$RPC = 1.96 \times Sd$$

Where Sd was calculated as the standard deviation of the differences between the IMU_{sys} and Qualisys measurements across all observations. The upper (ULA) and lower (LLA) limits of agreement were calculated as:

$$LA = M_{diff} \pm RPC$$

If a normal distribution could not be assumed, non-parametric adjustments were applied to the RPC calculation. The non-parametric repeatability coefficient (RPC_{np}) was calculated as (Peck et al., 2015):

$$RPC_{np} = 1.45 \times IQR$$

Where IQR is the interquartile range of the differences across observations.

CHAPTER IV - RESULTS

4.1. Participants

This section presents F-values and T-values of a T-test with 22 participants (adults and adolescents) for age, height, weight, leg length, knee width, and ankle width.

Table 4.1. *F-values and T-values for comparison by age (adults and adolescents).*

	F - value	**P - value**
Age	0.01	6.73
Height	0.01	0.03*
Weight	0.68	0.01**
Leg Length	0.1	0.01**
Knee Width	0.23	0.02*
Ankle Width	0.02	0.15*

$p < 0.05$*; $p < 0.01$**

4.2. Hip

Table 4.2. *Data are shown as mean and standard deviation of the coefficient of determination (r^2), the slope (m), the intercept [°] (b), the mean absolute error [°] (MAE), the root mean square error [°] (RMSE) for the left hip for adults (A) and pediatrics (P) at two time points between the Qualisys and IMU_{sys}.*

LEFT HIP

	Time Point 1					**Time Point 2**				
	r^2	**m**	**b**	**MAE**	**RMSE**	**r^2**	**m**	**b**	**MAE**	**RMSE**
A	0.97 ± 0.01	0.99 ± 0.05	0.54 ± 5.72	4.84 ± 2.89	5.29 ± 2.78	0.96 ± 0.02	0.97 ± 0.04	-0.12 ± 4.82	4.39 ± 2	4.92 ± 2.02
P	0.97 ± 0.02	0.95 ± 0.04	0.44 ± 7.37	6.69 ± 2.5	7.06 ± 2.41	0.96 ± 0.02	0.93 ± 0.06	-1.60 ± 8.79	7.63 ± 4.44	8.15 ± 4.23

Table 4.3. *Data are shown as mean and standard deviation of the mean difference [°] (Mdif), the mean difference standard deviation [°] (MdifSD), the upper limits of agreement [°] (LAU), the lower limits of agreement [°] (LAL), the difference in the limits of agreement [°] (DifLA), and the repeatability coefficient [°] (RPC) for the left hip for adults (A) and pediatrics (P) at two time points between the Qualisys and IMU$_{sys}$.*

LEFT HIP

	Time Point 1						Time Point 2					
	Mdif	**MdifSD**	**LAU**	**LAL**	**DifLA**	**RPC**	**Mdif**	**MdifSD**	**LAU**	**LAL**	**DifLA**	**RPC**
A	-0.36 ± 5.76	2.24 ± 0.51	3.94 ± 6.32	-4.66 ± 5.4	8.6 ± 2.32	4.3 ± 1.16	2.07 ± 4.8	2.60 ± 0.62	7.06 ± 4.62	-2.92 ± 5.33	9.98 ± 2.71	4.99 ± 1.36
P	-0.08 ± 7.39	2.29 ± 0.63	4.22 ± 7.35	-4.38 ± 7.62	8.60 ± 2.35	4.30 ± 1.18	2.07 ± 8.8	2.6 ± 0.74	7.06 ± 9.3	-2.92 ± 8.71	9.98 ± 3.88	4.99 ± 1.94

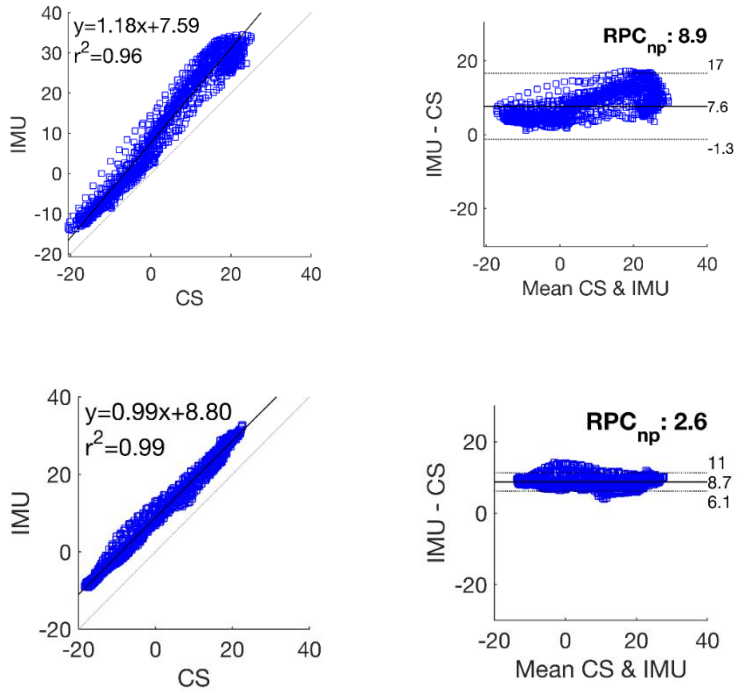

Figure 4.1. *Linear regression plots (left side) and Bland and Altman plots with 95% limits of agreement (right side) for the left hip. The top row illustrates the data for the participant with the highest RPC observed in the study; the bottom row illustrates the data for the participant with the lowest RPC observed in the study. IMU: IMU$_{sys}$, CS: Qualisys system.*

Table 4.4. *Data are shown as mean and standard deviation of the coefficient of determination (r^2), the slope (m), the intercept [°] (b), the mean absolute error [°] (MAE), the root mean square error [°] (RMSE) for the right hip for adults (A) and pediatrics (P) at two time points between the Qualisys and IMU_{sys}.*

RIGHT HIP

	Time Point 1					**Time Point 2**				
	r^2	**m**	**b**	**MAE**	**RMSE**	**r^2**	**m**	**b**	**MAE**	**RMSE**
A	0.97 ± 0.02	0.95 ± 0.07	-0.02 ± 6.8	5.45 ± 3.65	5.94 ± 3.53	0.96 ± 0.01	0.96 ± 0.06	-1.31 ± 6.91	5.71 ± 7.02	6.25 ± 7.49
P	0.96 ± 0.03	0.93 ± 0.05	2.01 ± 7.13	6.53 ± 3.29	7.01 ± 3.09	0.97 ± 0.02	0.92 ± 0.05	-0.10 ± 7.87	7.02 ± 3.91	7.49 ± 3.74

Table 4.5. *Data are shown as mean and standard deviation of the coefficient of the mean difference [°] (Mdif), the mean difference standard deviation [°] (MdifSD), the upper limits of agreement [°] (LAU), the lower limits of agreement [°] (LAL), the difference in the limits of agreement [°] (DifLA), and the repeatability coefficient [°] (RPC) for the right hip for adults (A) and pediatrics (P) at two time points between the Qualisys and IMU_{sys}.*

RIGHT HIP

	Time Point 1						**Time Point 2**					
	Mdif	**MdifSD**	**LAU**	**LAL**	**DifLA**	**RPC**	**Mdif**	**MdifSD**	**LAU**	**LAL**	**DifLA**	**RPC**
A	0.36 ± 6.76	2.38 ± 0.73	4.98 ± 6.83	-4.26 ± 6.89	9.25 ± 2.29	4.62 ± 1.14	1.88 ± 6.88	2.55 ± 0.42	6.24 ± 6.84	-2.49 ± 7.09	8.72 ± 2.22	4.36 ± 1.11
P	-1.55 ± 7.44	2.47 ± 0.7	3.16 ± 7.79	-6.26 ± 7.38	9.41 ± 2.93	4.71 ± 1.46	0.61 ± 8.28	2.55 ± 0.59	5.68 ± 8.74	-4.45 ± 8.13	10.13 ± 3.31	5.07 ± 1.65

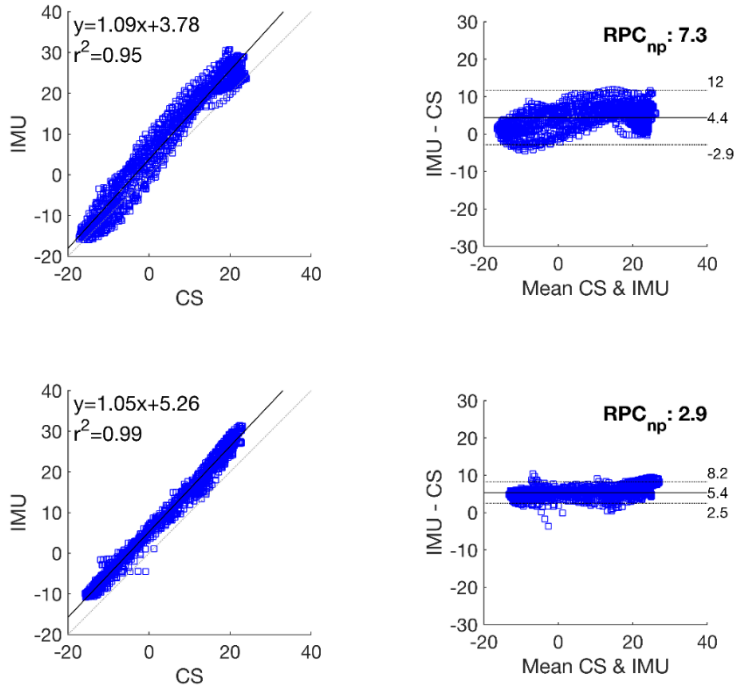

Figure 4.2. *Linear regression plots (left side) and Bland and Altman plots with 95% limits of agreement (right side) for the right hip. The top row illustrates the data for the participant with the highest RPC observed in the study; the bottom row illustrates the data for the participant with the lowest RPC observed in the study. IMU: IMU_{sys}, CS: Qualisys system.*

4.3. Knee

Table 4.6. *Data are shown as mean and standard deviation of the coefficient of determination (r^2), the slope (m), the intercept [°] (b), the mean absolute error [°] (MAE)) for the left knee for adults (A) and pediatrics (P) at two time points between the Qualisys and IMU_{sys}.*

LEFT KNEE

	Time Point 1					Time Point 2				
	r^2	**m**	**b**	**MAE**	**RMSE**	**r^2**	**m**	**b**	**MAE**	**RMSE**
A	0.96 ± 0.02	0.85 ± 0.04	-3 ± 7.16	8.41 ± 4.31	9.69 ± 4.04	0.95 ± 0.03	0.84 ± 0.05	-3.68 ± 6.72	9.24 ± 3.62	10.6 ± 3.42
P	0.95 ± 0.03	0.8 ± 0.09	-3.39 ± 4.31	9.15 ± 4.77	10.78 ± 4.84	0.95 ± 0.04	0.8 ± 0.12	-3.84 ± 5.14	9.6 ± 5.68	11.23 ± 5.85

Table 4.7. *Data are shown as mean and standard deviation of the coefficient of the mean difference [°] (Mdif), the mean difference standard deviation [°] (MdifSD), the upper limits of agreement [°] (LAU), the lower limits of agreement [°] (LAL), the difference in the limits of agreement [°] (DifLA), and the repeatability coefficient [°] (RPC) for the left knee for adults (A) and pediatrics (P) at two time points between the Qualisys and* IMU_{sys}.

LEFT KNEE

	Time Point 1						Time Point 2					
	Mdif	**MdifSD**	**LAU**	**LAL**	**DifLA**	**RPC**	**Mdif**	**MdifSD**	**LAU**	**LAL**	**DifLA**	**RPC**
A	4.46 ± 7.22	5.22 ± 0.89	12.69 ± 6.41	-3.77 ± 8.64	16.47 ± 4.8	8.23 ± 2.4	5.14 ± 6.9	5.51 ± 1.46	14.48 ± 6.13	-4.20 ± 8.51	18.67 ± 5.4	9.34 ± 2.7
P	6.53 ± 5.11	5.91 ± 1.86	17.72 ± 7.72	-4.67 ± 5.35	22.38 ± 8.49	11.19 ± 4.25	7.04 ± 6.01	5.9 ± 2.61	18.41 ± 9.14	-4.33 ± 7.07	22.74 ± 11.51	11.37 ± 5.75

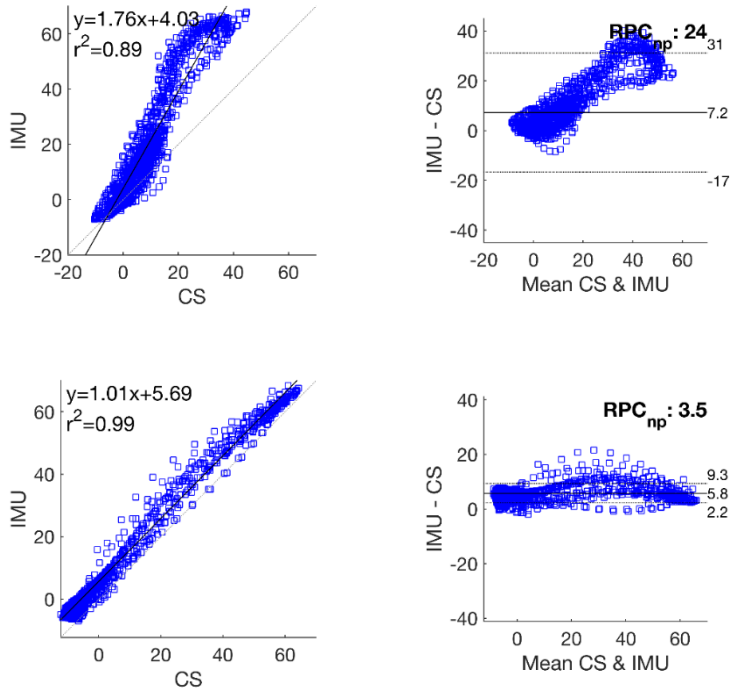

Figure 4.3. *Linear regression plots (left side) and Bland and Altman plots with 95% limits of agreement (right side) for the left knee. The top row illustrates the data for the participant with the highest RPC observed in the study; the bottom row illustrates the data for the participant with the lowest RPC observed in the study. IMU:* IMU_{sys}*, CS: Qualisys system.*

Table 4.8. *Data are shown as mean and standard deviation of the coefficient of determination (r^2), the slope (m), the intercept [°] (b), the mean absolute error [°] (MAE), the root mean square error [°] (RMSE) for the right knee for adults (A) and pediatrics (P) at two time points between the Qualisys and IMU_{sys}.*

RIGHT KNEE

	Time Point 1					Time Point 2				
	r^2	**m**	**b**	**MAE**	**RMSE**	**r^2**	**m**	**b**	**MAE**	**RMSE**
A	0.97 ± 0.03	0.86 ± 0.04	-3.31 ± 5.34	7.57 ± 3.6	8.64 ± 3.57	0.95 ± 0.03	0.86 ± 0.05	-4.56 ± 5.35	8.90 ± 4.16	10.22 ± 4.21
P	0.94 ± 0.06	0.82 ± 0.08	-0.51 ± 7.87	9.18 ± 4.25	10.38 ± 4.43	0.96 ± 0.02	0.83 ± 0.08	-2.29 ± 8.74	10.0 ± 4.71	11.23 ± 4.4

Table 4.9. *Data are shown as mean and standard deviation of the coefficient of the mean difference [°] (Mdif), the mean difference standard deviation [°] (MdifSD), the upper limits of agreement [°] (LAU), the lower limits of agreement [°] (LAL), the difference in the limits of agreement [°] (DifLA), and the repeatability coefficient [°] (RPC) for the right knee for adults (A) and pediatrics (P) at two time points between the Qualisys and IMU_{sys}.*

RIGHT KNEE

	Time Point 1						Time Point 2					
	Mdif	**MdifSD**	**LAU**	**LAL**	**DifLA**	**RPC**	**Mdif**	**MdifSD**	**LAU**	**LAL**	**DifLA**	**RPC**
A	4.83 ± 5.67	4.63 ± 1.4	12.95 ± 5.61	-3.29 ± 6.8	16.23 ± 5.17	8.12 ± 2.59	6.44 ± 5.84	5.41 ± 1.51	14.97 ± 7.07	-2.1 ± 5.36	17.07 ± 4.6	8.53 ± 2.3
P	2.77 ± 9.39	5.45 ± 1.87	12.44 ± 9.82	-6.89 ± 10.2	19.33 ± 6.96	9.66 ± 3.48	4.23 ± 9.83	5.33 ± 1.32	13.68 ± 10.34	-5.23 ± 10.19	18.92 ± 5.9	9.46 ± 2.95

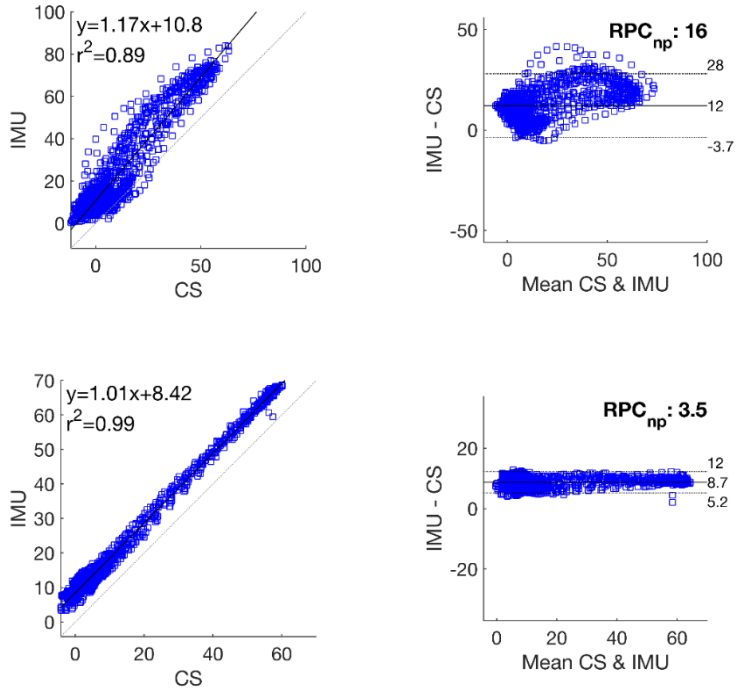

Figure 4.4. *Linear regression plots (left side) and Bland and Altman plots with 95% limits of agreement (right side) for the right knee. The top row illustrates the data for the participant with the highest RPC observed in the study; the bottom row illustrates the data for the participant with the lowest RPC observed in the study. IMU: IMU_{sys}, CS: Qualisys system.*

CHAPTER V – DISCUSSION

5.1. Linear regression

Our lowest average coefficient of determination (r^2) observed for the hip and knee across sides, age groups, and time points was 0.94. This indicates a strong relationship between the IMU_{sys} and the Qualisys for different anthropometric characteristics even after a relatively prolonged use of the systems. The values for r^2 reported in this study support previous validation studies of a IMU system (Xsens MVN BIOMECH) for the hip and knee ($r^2 > 0.9$) (Al-Amri et al., 2018; Zhang et al., 2013). Another study investigated the validity of hip flexion measurements by the akto-t system (Bessone et al., 2019) during a short walking trial in healthy participants over the age of 18; this study reported $r^2 > 0.9$.

The average *m* coefficients indicate a slight tendency (Adults: m = 0.95; Adolescents: m = 0.92) in the IMU_{sys} to overestimate hip flexion angles, particularly for adolescents. This overestimation increases for knee flexion angles (Adults: m = 0.84; Adolescents: m = 0.80). Additionally, although average *b* coefficients are close to zero, standard deviations (Hip Adults: $4.92 < b < 6.91$; Hip Adolescents: $7.13 < b < 8.79$; Knee Adults: $5.34 < b < 7.16$; Knee Adolescents: $4.31 < b < 8.74$) indicate large individual variability. This suggest a large variability with a central tendency near zero for fixed offsets, which is a clear limitation of the IMU_{sys}. When using the IMU_{sys}, the unpredictability of the offset makes it difficult to correct and apply across individuals. Future work should investigate techniques that can address this issue by providing individualized offset corrections.

5.2. Root mean square error

In our study, there was a significant difference between two groups in terms of age and anthropometric measures (Table 4.1.). Admittedly, muscular-skeletal growth influences gait features such as step frequency, step length, and walking velocity (Todd et al., 1989). A spatial-temporal gait study (Lythgo et al., 2009) found that the non-normalized measures of gait speed, step length, stride length, step time and stride time increased with age, but cadence reduced with age. This means that age related limb length changes influence specific gait features. However, it seems that the validity of the IMU_{sys} was not largely affected by physical changes or different segment proportion. The RMSEs and standard deviations observed for the hip across sides and time points in adults were relatively similar with the RMSEs and standard deviations for the hip in pediatrics (table 4.2. and 4.3.). Also, relatively similar RMSEs and standard deviations for the knee across sides and time points between age groups were found (table 4.4 and 4.5). However, the RMSE reported for the knee in our study (the smallest knee RMSE in adolescents: 10.38°; the smallest knee RMSE in adults: 8.6°) was larger than the values reported by Bessone et al. (2019) (6.8°), particularly in pediatrics. One possible explanation about the relatively larger error for the knee can be related to age groups. Bessone et al. (2019) did not test pediatrics. Therefore, the cause of error for the knee joint motions in pediatrics should be worth investigating.

5.3. The mean of differences and repeatability coefficient

The Mdif (< |1.9|°) and RPC (< 4.7°) for the hip in adults across sides and time points were lower than the Mdif (> |4.5|°) and RPC (> 8.1°) for the knee in adults. Similar

results were observed in the pediatrics group (Hip: Mdif < |2.1|°, RPC <5°; Knee: Mdif > |2.8|°, RPC > 9.5°). Bessone et al. (2019), when validating the aktos-t IMU system against a CBMC (Vicon Motion Systems), established an acceptable 'bias' (Mdif) for biomechanical research when smaller than 5° (El-Zayat et al., 2013; Schiefer et al., 2014), and interpreted the RPC as not precise when larger than 10° (El-Zayat et al., 2013; Schiefer et al., 2014). The Mdif for the hip across sides, age groups, and time points in our study fell within the acceptable range, but standard deviations indicated large variability (< 8.8°). The RPC for the hip across sides, age groups, and time points was considered precise (< 5°). The Mdif for the knee across sides, age groups, and time points was close to 5°, but standard deviations indicated large variability (< 9.8°). The RPC for the knee across sides, age groups, and time points was considered precise except for the left knee across time points in pediatrics (> 11.19°).

Differences in 'bias' and RPC between the hip and the knee might be explained by the different ranges of motion (ROM) of these joints during gait. Generally, the ROM for the knee is larger than the ROM for the hip, meaning that the larger ROM can result in larger variability in errors. Figure 4.3 illustrates the magnitude of errors across the ROM of the knee. There was a tendency to increase 'bias' as the excursion of the knee angle is larger. This means that when the knee is extended, the bias is very small while when the knee is flexed, the bias is very large. However, we could not find any similar tendency for the hip.

5.4. Clinical relevance

Clinical relevance indicates what the results of a study mean in clinical settings. In this section, we investigated how the results of our IMU_{sys} study could be interpreted on clinical practice.

A gait patterns study (Delval et al,. 2008) of patients with Parkinson's disease (PD) and healthy subjects (HS) reported an average 12 degrees of hip flexion deviation between PD and HS during late stance phase (terminal stance and pre-swing phases) and an average 9 degrees of knee flexion deviation during mid swing phase. The hip deviation (12°) that PD have can be easily detected by our IMU_{sys} that has relatively small deviation (RMSE: 8.1°±4.2, Mdif: 2.1°±8.8, RPC: 5°±2). However, it would be hard to say that the PD's knee deviant pattern (9°) would be detected by our IMU_{sys} because the PD's knee deviation is close to or within the range of the knee deviation (RMSE: 8.6°±3.6, Mdif: 2.8°±9.4, RPC: 8.1°±2.6) for our IMU_{sys}. Therefore, the errors for the hip reported in our study support the use of our IMU_{sys} in clinical settings that evaluate patients with PD. Another gait analysis study (Carmo et al., 2012) that compared post-stroke (PS) and healthy gait reported an average of 5.9 degrees of deviation for the hip extension, and an average 17.4 degrees for the knee flexion. Based on our data, it would be difficult to identify the hip pattern (5.9°) in patients with PS with our IMU_{sys}. On the other hand, the errors reported in our study support the use of the IMU_{sys} in detecting the knee pattern in patients with PS.

5.5. Limitations

The current study presents several limitations. The possibility of comparing the results of this study with the literature is limited due to the specific biomechanical models applied to calculate joints angles using the IMU_{sys} and CBMC. Although IMU systems and CBMC define body segments of interest and calculate changes in the orientations of the body segments in reference to a calibration position, the sensor placement defined by each model might be different and result in different models. For example, the hip joint center might be defined differently depending on the models (e.g. the PIG model: Davis regression equations).

Another limitation of our study concerns that 20 seconds of the 1-minute walking for each participant were analyzed. A participant with a less consistent gait pattern could have more or less trials in strides than another participant with a more consistent gait pattern could have. In particular, the pediatric group's gait pattern may not be more consistent than the adults' gait pattern is. Namely, the entire 20 seconds for each participant could not be considered as comparing the completely same gait pattern or number of strides of each participant. Therefore, this limitation can add an element of variability into our results.

The other limitation concerns the actual gait speed that individuals performed on the treadmill. Even though the treadmill ran at a self-selected speed for each participant, there might be small variation in the participant's speed during the trial.

CHAPTER VI - CONCLUSION

The purpose of this study was to determine the accuracy of an IMU_{sys} for calculating hip and knee flexion angles during gait in both adults and pediatrics at two different time points. In our study, a strong relationship ($r^2 > 0.94$) between our IMU_{sys} and Qualisys was found. Average *b* coefficients were close to zero, but with large variability across participants. RMSE, Mdif, and RPC values were maintained during prolonged use of the IMU_{sys} across individuals with different anthropometry. However, large errors were observed for the knee joint motions in pediatrics. The use of the IMU_{sys} in the clinical settings to evaluate the hip for patients with Parkinson's disease and the knee for patients with post-stroke might be considered.

Future work should focus on: 1) developing techniques that can address the large variability of offsets across individuals, 2) identifying the phases in the gait cycle with larger deviations from the IMU_{sys} and, 3) what are the causes of such deviations.

Appendix A

Table 7.1. *The results for the left hip across age groups and time points*

LEFT HIP

	Time Point 1											Time Point 2										
A	**r^2**	**m**	**b**	**MAE**	**RMSE**	**Mdif**	**MdifSD**	**LAU**	**LAL**	**DifLA**	**RPC**	**r^2**	**m**	**b**	**MAE**	**RMSE**	**Mdif**	**MdifSD**	**LAU**	**LAL**	**DifLA**	**RPC**
1	0.98	1.00	-4.60	4.64	5.00	5.22	1.92	9.52	0.91	8.61	4.31	0.99	0.99	-4.45	4.56	4.81	4.92	1.56	8.05	1.79	6.27	3.13
2	0.95	1.07	-2.79	2.96	3.58	2.47	2.87	8.13	-3.19	11.31	5.66	0.95	1.06	-2.35	2.86	3.47	1.91	2.97	8.06	-4.24	12.29	6.15
3	0.94	0.97	-9.16	9.39	9.81	9.69	2.88	14.36	5.03	9.33	4.67	0.92	0.94	-5.84	6.35	7.02	6.29	3.50	11.48	1.10	10.38	5.19
4	0.96	0.94	8.49	8.22	8.69	-8.35	2.90	-3.96	-12.74	8.78	4.39	0.94	0.94	9.52	9.25	9.89	-8.65	3.51	-1.16	-16.13	14.97	7.49
5	0.98	1.03	1.96	2.45	2.87	-2.30	1.80	0.33	-4.92	5.26	2.63	0.97	1.02	2.72	2.95	3.51	-2.49	1.96	1.16	-6.14	7.30	3.65
6	0.99	0.99	9.18	9.10	9.20	-9.01	1.35	-6.37	-11.66	5.30	2.65	0.96	0.94	3.59	3.26	3.91	-2.90	2.33	0.68	-6.48	7.15	3.58
7	0.97	0.95	3.26	2.80	3.33	-2.56	1.98	1.06	-6.18	7.25	3.62	0.96	0.96	4.11	3.66	4.22	-3.78	2.26	1.25	-8.81	10.06	5.03
8	0.96	0.91	-0.21	2.21	2.83	0.59	2.66	7.08	-5.90	12.98	6.49	0.96	0.92	-2.78	3.68	4.32	3.52	2.52	8.64	-1.61	10.26	5.13
9	0.98	1.03	-3.62	3.50	3.99	3.44	2.18	7.42	-0.53	7.95	3.98	0.98	1.01	3.75	3.82	4.21	-3.85	1.80	-0.93	-6.76	5.83	2.91
10	0.98	0.97	-1.82	2.27	2.74	1.98	1.84	5.60	-1.64	7.24	3.62	0.97	0.96	-4.91	5.24	5.69	5.05	2.23	9.39	0.72	8.67	4.33
11	0.98	1.05	7.73	7.81	8.06	-7.52	1.98	-3.43	-11.61	8.18	4.09	0.96	0.97	-4.77	5.42	5.83	5.68	2.65	9.37	1.99	7.38	3.69
12	0.95	0.95	-1.98	2.77	3.43	2.01	2.56	7.52	-3.49	11.01	5.51	0.96	0.95	0.00	1.63	2.14	0.25	2.12	3.85	-3.34	7.19	3.60
M	0.97	0.99	0.54	4.84	5.29	-0.36	2.24	3.94	-4.66	8.60	4.30	0.96	0.97	-0.12	4.39	4.92	0.50	2.45	4.99	-3.99	8.98	4.49
SD	0.01	0.05	5.72	2.89	2.78	5.76	0.51	6.32	5.40	2.32	1.16	0.02	0.04	4.82	2.00	2.02	4.80	0.62	4.62	5.33	2.71	1.36
	Time Point 1											**Time Point 2**										
P	**r^2**	**m**	**b**	**MAE**	**RMSE**	**Mdif**	**MdifSD**	**LAU**	**LAL**	**DifLA**	**RPC**	**r^2**	**m**	**b**	**MAE**	**RMSE**	**Mdif**	**MdifSD**	**LAU**	**LAL**	**DifLA**	**RPC**
13	0.97	0.97	5.33	5.09	5.56	-5.20	2.51	-0.81	-9.58	8.77	4.38	0.96	0.81	-6.06	8.15	8.96	7.64	3.72	16.57	-1.29	17.86	8.93
14	0.95	0.94	5.13	4.75	5.29	-4.78	2.58	-0.13	-9.44	9.31	4.65	0.95	0.95	7.44	7.11	7.70	-6.69	2.96	-1.54	-11.84	10.31	5.15
15	0.99	0.93	8.40	8.21	8.38	-8.22	1.69	-4.57	-11.87	7.30	3.65	0.99	0.92	11.96	12.17	12.36	-12.31	2.16	-7.90	-16.73	8.83	4.42
16	0.95	0.91	3.16	3.39	3.88	-2.48	3.10	2.82	-7.78	10.59	5.30	0.97	0.94	-0.37	1.75	2.49	0.55	2.31	3.68	-2.58	6.26	3.13
17	0.97	0.88	-6.18	7.99	8.45	7.90	2.76	13.72	2.07	11.65	5.83	0.96	0.86	-3.65	4.89	5.88	4.32	3.40	11.23	-2.60	13.83	6.92
18	0.98	0.98	2.88	2.71	3.12	-2.61	1.70	0.50	-5.72	6.22	3.11	0.95	0.92	2.63	1.90	2.64	-0.96	2.26	2.85	-4.77	7.62	3.81
19	0.99	0.99	-8.73	8.79	8.92	8.71	1.51	11.27	6.14	5.13	2.56	0.99	1.02	-14.30	14.03	14.11	14.27	1.53	17.07	11.47	5.60	2.80
20	0.99	0.98	-8.81	8.97	9.08	8.81	1.44	11.72	5.90	5.83	2.91	0.98	0.96	-6.56	6.78	6.97	6.37	1.63	9.78	2.96	6.82	3.41

Table 7.1. Continued

21	0.93	0.98	-7.09	7.31	7.82	6.96	2.80	12.57	1.34	11.23	5.61	0.93	0.99	-13.37	13.64	14.02	13.58	3.24	20.06	7.11	12.95	6.47
22	0.97	0.90	10.29	9.72	10.12	-9.86	2.83	-4.86	-14.86	10.00	5.00	0.97	0.89	6.27	5.83	6.40	-6.06	2.76	-1.18	-10.93	9.75	4.88
M	0.97	0.95	0.44	6.69	7.06	-0.08	2.29	4.22	-4.38	8.60	4.30	0.96	0.93	-1.60	7.63	8.15	2.07	2.60	7.06	-2.92	9.98	4.99
SD	0.02	0.04	7.37	2.50	2.41	7.39	0.63	7.35	7.62	2.35	1.18	0.02	0.06	8.79	4.44	4.23	8.80	0.74	9.30	8.71	3.88	1.94

Table 7.2. *The results for the right hip across age groups and time points*

	RIGHT HIP																				
	Time Point 1											**Time Point 2**									
A	r^2	**m**	**b**	**MAE**	**RMSE**	**Mdif**	**MdifSD**	**LAU**	**LAL**	**DifLA**	**RPC**	r^2	**m**	**b**	**MAE**	**RMSE**	**Mdif**	**MdifSD**	**LAU**	**LAL**	**DifLA**	**RPC**
1	0.97	1.05	-7.57	7.12	7.45	7.69	2.20	12.89	2.50	10.39	5.20	0.98	1.05	-7.33	6.93	7.21	7.35	2.07	10.26	4.45	5.82	2.91
2	0.98	1.02	-5.06	4.84	5.18	4.77	1.86	8.63	0.91	7.72	3.86	0.97	1.00	-3.99	4.04	4.58	4.00	2.34	7.76	0.25	7.52	3.76
3	0.94	1.02	-12.67	12.50	12.86	12.71	3.03	18.08	7.35	10.72	5.36	0.94	1.01	-15.40	15.33	15.63	16.20	3.06	20.80	11.60	9.20	4.60
4	0.92	0.84	4.17	4.14	5.33	-3.02	4.29	3.72	-9.76	13.47	6.74	0.95	0.86	6.04	5.21	6.16	-5.14	3.46	2.21	-12.48	14.69	7.34
5	0.98	0.93	3.71	3.25	3.78	-3.48	2.31	1.51	-8.47	9.99	4.99	0.97	0.95	4.37	4.00	4.55	-3.91	2.31	0.07	-7.89	7.96	3.98
6	0.97	0.93	9.22	8.93	9.14	-9.13	1.97	-5.39	-12.87	7.48	3.74	0.95	0.93	3.47	3.22	3.90	-2.86	2.45	0.69	-6.41	7.10	3.55
7	0.97	0.94	2.65	2.26	3.03	-1.60	2.34	2.28	-5.48	7.76	3.88	0.97	0.96	3.25	2.87	3.51	-2.39	2.16	1.25	-6.04	7.29	3.65
8	0.98	0.86	-0.99	2.89	3.61	2.26	2.63	8.13	-3.62	11.74	5.87	0.98	0.86	-3.79	5.38	5.88	4.96	2.38	9.90	0.02	9.88	4.94
9	0.97	0.99	-0.51	1.71	2.16	0.38	2.08	4.67	-3.91	8.58	4.29	0.95	0.96	6.26	6.19	6.78	-5.89	2.80	-1.75	-10.04	8.29	4.14
10	0.99	0.94	-4.88	5.48	5.72	5.37	1.67	8.24	2.50	5.74	2.87	0.96	0.99	-10.15	10.30	10.60	10.44	2.50	15.17	5.71	9.46	4.73
11	0.97	0.91	10.78	10.79	11.09	-10.92	2.56	-5.56	-16.28	10.72	5.36	0.95	0.93	-0.63	2.61	3.17	1.70	2.90	6.47	-3.07	9.54	4.77
12	0.98	1.02	0.94	1.46	1.93	-0.72	1.64	2.58	-4.03	6.62	3.31	0.96	0.99	2.13	2.41	2.96	-1.96	2.13	2.00	-5.92	7.92	3.96
M	0.97	0.95	-0.02	5.45	5.94	0.36	2.38	4.98	-4.26	9.25	4.62	0.96	0.96	-1.31	5.71	6.25	1.88	2.55	6.24	-2.49	8.72	4.36
SD	0.02	0.07	6.80	3.65	3.53	6.76	0.73	6.83	6.89	2.29	1.14	0.01	0.06	6.91	3.77	3.66	6.88	0.42	6.84	7.09	2.22	1.11

Table 7.2. Continued

	TIME POINT 1											TIME POINT 2										
P	r^2	**m**	**b**	**MAE**	**RMSE**	**Mdif**	**MdifSD**	**LAU**	**LAL**	**DifLA**	**RPC**	r^2	**m**	**b**	**MAE**	**RMSE**	**Mdif**	**MdifSD**	**LAU**	**LAL**	**DifLA**	**RPC**
13	0.95	0.97	4.96	5.01	5.54	-5.10	3.11	-0.24	-9.96	9.72	4.86	0.95	0.87	-3.06	4.56	5.36	4.42	3.33	11.70	-2.85	14.55	7.28
14	0.96	0.81	-0.93	3.72	4.78	2.72	3.64	9.93	-4.49	14.41	7.21	0.95	0.88	0.51	2.74	3.42	-0.19	3.40	6.67	-7.05	13.73	6.86
15	0.99	0.95	7.62	7.41	7.65	-7.13	1.89	-3.60	-10.66	7.05	3.53	0.99	0.95	8.82	8.80	8.97	-8.63	1.74	-5.42	-11.83	6.41	3.21
16	0.97	0.93	9.70	9.46	9.68	-9.94	2.05	-6.81	-13.07	6.26	3.13	0.98	0.91	5.29	4.87	5.33	-4.78	2.16	-1.64	-7.91	6.26	3.13
17	0.97	1.01	4.21	4.29	4.88	-3.93	2.42	0.92	-8.78	9.70	4.85	0.96	1.04	6.91	6.82	7.37	-7.03	2.89	-0.55	-13.52	12.97	6.48
18	0.97	0.93	0.30	1.67	2.15	0.67	2.05	4.02	-2.68	6.70	3.35	0.95	0.93	-1.87	3.01	3.81	2.20	2.36	5.69	-1.29	6.98	3.49
19	0.99	0.94	-8.94	9.40	9.54	9.26	1.59	12.82	5.70	7.12	3.56	0.98	0.90	-13.83	14.93	15.08	14.91	2.12	20.21	9.62	10.59	5.29
20	0.98	0.90	-6.42	7.05	7.31	6.90	1.93	11.06	2.74	8.31	4.16	0.98	0.92	-3.82	4.39	4.71	4.44	1.87	7.67	1.21	6.46	3.23
21	0.88	0.93	-3.41	4.65	5.61	4.20	3.41	11.17	-2.77	13.94	6.97	0.95	0.94	-9.62	10.87	11.26	10.56	2.95	16.70	4.41	12.28	6.14
22	0.97	0.93	13.03	12.65	12.91	-13.13	2.60	-7.68	-18.58	10.91	5.45	0.97	0.92	9.63	9.24	9.61	-9.79	2.67	-4.26	-15.33	11.08	5.54
M	0.96	0.93	2.01	6.53	7.01	-1.55	2.47	3.16	-6.26	9.41	4.71	0.97	0.92	-0.10	7.02	7.49	0.61	2.55	5.68	-4.45	10.13	5.07
SD	0.03	0.05	7.13	3.29	3.09	7.44	0.70	7.79	7.38	2.93	1.46	0.02	0.05	7.87	3.91	3.74	8.28	0.59	8.74	8.13	3.31	1.65

Table 7.3. *The results for the left knee across age groups and time points*

	LEFT KNEE																					
	Time Point 1											Time Point 2										
A	r^2	**m**	**b**	**MAE**	**RMSE**	**Mdif**	**MdifSD**	**LAU**	**LAL**	**DifLA**	**RPC**	r^2	**m**	**b**	**MAE**	**RMSE**	**Mdif**	**MdifSD**	**LAU**	**LAL**	**DifLA**	**RPC**
1	0.97	0.82	8.66	6.76	7.29	-7.29	5.13	1.05	-15.64	16.69	8.35	0.99	0.81	8.67	5.98	6.67	-6.55	4.96	5.19	-18.28	23.47	11.74
2	0.94	0.87	-7.45	10.94	12.03	9.62	5.01	16.58	2.66	13.92	6.96	0.92	0.83	-7.36	12.06	13.34	10.00	5.70	17.52	2.49	15.03	7.51
3	0.95	0.82	-7.79	10.92	12.53	9.01	6.25	19.58	-1.56	21.15	10.57	0.93	0.86	-6.34	9.32	11.00	7.26	6.88	15.57	-1.04	16.61	8.30
4	0.93	0.80	7.82	7.31	8.74	-6.64	7.30	7.05	-20.33	27.38	13.69	0.88	0.82	8.80	8.65	10.16	-8.37	8.14	3.21	-19.95	23.17	11.58
5	0.97	0.93	-4.77	5.69	6.82	5.24	3.85	9.80	0.67	9.13	4.57	0.99	0.98	-5.46	5.76	6.35	5.78	2.73	9.33	2.23	7.09	3.55
6	0.97	0.83	-0.15	3.45	5.56	0.81	4.76	7.39	-5.78	13.17	6.59	0.97	0.81	-0.37	4.29	6.51	1.19	5.39	12.29	-9.92	22.22	11.11
7	0.95	0.87	-11.27	14.30	15.21	12.66	5.21	20.23	5.09	15.14	7.57	0.97	0.84	-9.77	13.60	14.62	11.60	5.38	21.64	1.56	20.08	10.04
8	0.98	0.80	-0.42	4.76	6.48	3.30	5.05	12.52	-5.91	18.43	9.21	0.97	0.79	0.02	4.45	6.47	1.90	5.21	13.76	-9.95	23.71	11.86

Table 7.3. Continued

9	0.98	0.89	-10.83	13.35	14.03	12.38	4.32	17.83	6.93	10.90	5.45	0.98	0.86	-9.84	13.02	13.94	11.28	4.97	19.85	2.72	17.13	8.57
10	0.97	0.82	-0.11	4.12	5.93	2.09	4.75	11.04	-6.87	17.91	8.95	0.93	0.80	-4.14	7.66	9.87	5.59	6.38	14.77	-3.60	18.36	9.18
11	0.97	0.85	2.45	4.07	5.46	-1.16	5.41	7.84	-10.16	18.00	9.00	0.94	0.83	-7.59	13.16	14.78	9.98	6.85	22.51	-2.55	25.06	12.53
12	0.95	0.85	-12.13	15.19	16.17	13.49	5.54	21.38	5.60	15.78	7.89	0.99	0.88	-10.72	12.99	13.47	12.02	3.56	18.08	5.95	12.13	6.07
M	0.96	0.85	-3.00	8.41	9.69	4.46	5.22	12.69	-3.77	16.47	8.23	0.95	0.84	-3.68	9.24	10.60	5.14	5.51	14.48	-4.20	18.67	9.34
SD	0.02	0.04	7.16	4.31	4.04	7.22	0.89	6.41	8.64	4.80	2.40	0.03	0.05	6.72	3.62	3.42	6.90	1.46	6.13	8.51	5.40	2.70
	Time Point 1											**Time Point 2**										
P	r^2	**m**	**b**	**MAE**	**RMSE**	**Mdif**	**MdifSD**	**LAU**	**LAL**	**DifLA**	**RPC**	r^2	**m**	**b**	**MAE**	**RMSE**	**Mdif**	**MdifSD**	**LAU**	**LAL**	**DifLA**	**RPC**
13	0.90	0.71	0.10	7.49	10.39	4.71	7.38	18.03	-8.62	26.64	13.32	0.89	0.51	-1.11	11.11	15.47	7.21	11.22	31.11	-16.68	47.79	23.89
14	0.93	0.75	2.78	5.81	7.87	0.99	7.16	16.64	-14.67	31.31	15.66	0.93	0.75	3.43	5.90	8.11	1.27	7.50	15.75	-13.22	28.97	14.49
15	0.98	0.86	-5.77	9.20	10.06	8.15	4.06	17.02	-0.72	17.73	8.87	0.98	0.87	-6.44	9.51	10.29	8.75	3.91	15.98	1.52	14.46	7.23
16	0.94	0.82	-2.31	6.00	8.46	3.09	6.52	12.16	-5.98	18.13	9.07	0.97	0.85	-2.47	5.66	7.58	3.58	5.29	11.40	-4.24	15.64	7.82
17	0.95	0.83	-6.94	11.86	12.81	10.51	4.86	19.73	1.30	18.43	9.22	0.96	0.84	-4.94	9.57	10.72	8.40	4.89	19.74	-2.95	22.68	11.34
18	0.96	0.87	-2.72	5.55	6.97	4.19	4.63	12.02	-3.65	15.66	7.83	0.97	0.88	-0.51	2.88	4.33	1.29	3.66	6.09	-3.51	9.60	4.80
19	0.97	0.85	-11.47	14.49	15.23	13.09	4.68	22.19	3.99	18.20	9.10	0.99	0.89	-13.90	16.24	16.64	15.37	3.60	23.34	7.40	15.94	7.97
20	0.99	0.89	1.88	2.88	3.50	-1.28	3.50	5.36	-7.91	13.27	6.64	0.99	0.88	1.83	3.10	3.71	-1.25	3.71	6.52	-9.02	15.55	7.77
21	0.91	0.60	-4.66	18.76	21.00	14.28	9.45	34.81	-6.26	41.07	20.53	0.90	0.66	-7.89	20.73	22.63	17.12	9.08	34.32	-0.08	34.40	17.20
22	0.93	0.83	-4.78	9.42	11.47	7.53	6.88	19.21	-4.15	23.36	11.68	0.96	0.82	-6.41	11.32	12.84	8.68	6.11	19.85	-2.50	22.35	11.18
M	0.95	0.80	-3.39	9.15	10.78	6.53	5.91	17.72	-4.67	22.38	11.19	0.95	0.80	-3.84	9.60	11.23	7.04	5.90	18.41	-4.33	22.74	11.37
SD	0.03	0.09	4.31	4.77	4.84	5.11	1.86	7.72	5.35	8.49	4.25	0.04	0.12	5.14	5.68	5.85	6.01	2.61	9.41	7.07	11.51	5.75

Table 7.4. *The results for the right knee across age groups and time points*

	RIGHT KNEE																				
	Time Point 1											**Time Point 2**									
A	r^2	**m**	**b**	**MAE**	**RMSE**	**Mdif**	**MdifSD**	**LAU**	**LAL**	**DifLA**	**RPC**	r^2	**m**	**b**	**MAE**	**RMSE**	**Mdif**	**MdifSD**	**LAU**	**LAL**	**DifLA**	**RPC**
1	0.97	0.89	1.78	2.60	3.64	-0.63	3.64	3.60	-4.86	8.46	4.23	0.97	0.86	2.78	3.46	4.51	-1.48	4.50	5.73	-8.69	14.42	7.21
2	0.98	0.83	-9.26	13.69	14.29	12.21	4.09	20.18	4.24	15.94	7.97	0.97	0.81	-8.68	13.44	14.28	11.93	4.81	21.94	1.93	20.00	10

Table 7.4. Continued

3	0.94	0.88	-11.97	14.09	15.25	13.59	5.82	23.01	4.17	18.83	9.42	0.89	0.76	-13.51	18.35	20.28	16.46	8.63	30.83	2.09	28.73	14.37
4	0.91	0.87	2.55	5.29	6.84	-2.05	6.84	8.86	-12.95	21.81	10.9	0.88	0.83	6.37	7.12	8.71	-5.23	8.08	4.88	-15.34	20.22	10.11
5	0.99	0.9	-3.71	5.52	6.28	4.83	3.32	10.59	-0.94	11.53	5.76	0.95	0.88	-2.93	5.72	7.37	4.15	5.64	10.22	-1.92	12.14	6.07
6	0.97	0.85	-2.15	4.82	6.44	3.28	4.47	11.88	-5.33	17.21	8.60	0.97	0.86	-2.78	5.45	7.03	4.01	4.62	12.83	-4.81	17.64	8.82
7	0.97	0.82	-6.84	10.75	12.09	9.08	5.57	18.93	-0.76	19.70	9.85	0.98	0.86	-8.6	11.65	12.38	10.67	4.19	17.56	3.78	13.78	6.89
8	0.98	0.89	-4.13	6.43	7.24	6.38	3.32	12.75	0.00	12.75	6.38	0.98	0.85	-3.12	6.21	7.56	5.95	4.34	14.37	-2.46	16.83	8.41
9	0.98	0.84	-5.78	8.9	10.26	7.06	5.12	15.74	-1.62	17.36	8.68	0.96	0.86	-6.2	9.04	10.79	7.37	6.03	15.21	-0.47	15.67	7.84
10	0.98	0.9	-2.96	4.91	5.85	4.16	3.26	10.01	-1.69	11.70	5.85	0.95	0.94	-8.61	9.63	10.72	9.00	4.72	16.40	1.59	14.81	7.41
11	0.94	0.8	7.64	7.04	8.03	-5.94	6.96	7.51	-19.39	26.90	13.45	0.97	0.83	-5.31	10.53	11.83	9.14	5.39	18.46	-0.17	18.63	9.32
12	0.99	0.9	-4.82	6.83	7.52	5.99	3.15	12.30	-0.33	12.63	6.32	0.98	0.92	-4.19	6.16	7.15	5.26	3.92	11.24	-0.72	11.96	5.98
M	0.97	0.86	-3.31	7.57	8.64	4.83	4.63	12.95	-3.29	16.23	8.12	0.95	0.86	-4.56	8.90	10.22	6.44	5.41	14.97	-2.10	17.07	8.53
SD	0.03	0.04	5.34	3.60	3.57	5.67	1.40	5.61	6.80	5.17	2.59	0.03	0.05	5.35	4.16	4.21	5.84	1.51	7.07	5.36	4.60	2.30
	Time Point 1											**Time Point 2**										
P	r^2	**m**	**b**	**MAE**	**RMSE**	**Mdif**	**MdifSD**	**LAU**	**LAL**	**DifLA**	**RPC**	r^2	**m**	**b**	**MAE**	**RMSE**	**Mdif**	**MdifSD**	**LAU**	**LAL**	**DifLA**	**RPC**
13	0.89	0.80	2.73	4.64	6.56	0.24	6.42	10.37	-9.89	20.25	10.13	0.94	0.71	-3.25	9.62	11.84	7.52	6.90	21.62	-6.58	28.20	14.1
14	0.89	0.76	-6.91	12.93	15.14	12.17	8.07	27.99	-3.65	31.64	15.82	0.94	0.81	-6.25	11.30	12.93	10.66	6.31	22.94	-1.62	24.56	12.28
15	0.99	0.98	-8.13	8.60	8.77	8.74	1.72	12.24	5.23	7.01	3.50	0.97	0.98	-11.01	11.46	11.93	11.40	3.32	16.39	6.41	9.98	4.99
16	0.98	0.81	11.09	9.83	10.77	-11.52	5.07	-2.55	-20.5	17.95	8.97	0.97	0.85	10.34	9.17	9.96	-10.15	4.82	-2.07	-18.24	16.18	8.09
17	0.98	0.75	9.31	8.42	9.33	-9.79	5.97	2.64	-22.22	24.86	12.43	0.95	0.78	9.52	9.1	10.04	-9.84	7.10	2.75	-22.43	25.17	12.59
18	0.98	0.82	-2.76	6.52	8.15	4.52	4.90	14.13	-5.08	19.21	9.61	0.94	0.75	-1.16	5.17	7.42	3.10	5.80	11.44	-5.23	16.66	8.33
19	0.97	0.85	-12.77	15.58	16.27	13.82	4.68	19.63	8.00	11.63	5.82	0.98	0.88	-14.96	17.51	17.92	16.07	3.80	23.72	8.42	15.30	7.65
20	0.98	0.87	5.93	5.08	5.52	-5.20	4.21	2.42	-12.83	15.24	7.62	0.98	0.88	5.39	4.47	4.92	-4.48	3.88	2.33	-11.3	13.63	6.81
21	0.8	0.7	-4.75	15.56	17.52	13.30	8.07	24.54	2.07	22.48	11.24	0.94	0.82	-10.80	17.49	18.34	16.01	5.53	27.53	4.5	23.04	11.52
22	0.97	0.85	1.12	4.61	5.78	1.44	5.38	12.96	-10.07	23.03	11.52	0.96	0.87	-0.75	4.70	6.99	1.97	5.79	10.2	-6.26	16.46	8.23
M	0.94	0.82	-0.51	9.18	10.38	2.77	5.45	12.44	-6.89	19.33	9.66	0.96	0.83	-2.29	10	11.23	4.23	5.33	13.68	-5.23	18.92	9.46
SD	0.06	0.08	7.87	4.25	4.43	9.39	1.87	9.82	10.20	6.96	3.48	0.02	0.08	8.74	4.71	4.40	9.83	1.32	10.34	10.19	5.90	2.95

REFERENCES

Abdel-Aziz, Y. I., & Karara, H. M. (2015). Direct linear transformation from comparator coordinates into object space coordinates in close-range photogrammetry. *Photogrammetric Engineering and Remote Sensing*. https://doi.org/10.14358/PERS.81.2.103

Agustsson, A., Gislason, M. K., Ingvarsson, P., Rodby-Bousquet, E., & Sveinsson, T. (2019). Validity and reliability of an iPad with a three-dimensional camera for posture imaging. *Gait and Posture*. https://doi.org/10.1016/j.gaitpost.2018.12.018

Al-Amri, M., Nicholas, K., Button, K., Sparkes, V., Sheeran, L., & Davies, J. L. (2018). Inertial measurement units for clinical movement analysis: Reliability and concurrent validity. *Sensors (Switzerland)*. https://doi.org/10.3390/s18030719

Allard, P., Stokes, I. A. F., & Blanchi, J.-P. (1995). *Three-dimensional analysis of human movement*. Human Kinetics Publishers.

Aloba, A., Luc, A., Woodward, J., Dong, Y., Zhang, R., Jain, E., & Anthony, L. (2019). Quantifying Differences Between Child and Adult Motion Based on Gait Features. *Lecture Notes in Computer Science (Including Subseries Lecture Notes in Artificial Intelligence and Lecture Notes in Bioinformatics)*. https://doi.org/10.1007/978-3-030-23563-5_31

Aurand, A. M., Dufour, J. S., & Marras, W. S. (2017). Accuracy map of an optical motion capture system with 42 or 21 cameras in a large measurement volume. *Journal of Biomechanics*. https://doi.org/10.1016/j.jbiomech.2017.05.006

Baker, R., Leboeuf, F., Reay, J., & Sangeux, M. (2017). The Conventional Gait Model - Success and Limitations. In *Handbook of Human Motion*. https://doi.org/10.1007/978-3-319-30808-1_25-2

Beck, R. J., Andriacchi, T. P., Kuo, K. N., Fermier, R. W., & Galante, J. O. (1981). Changes in the gait patterns of growing children. *Journal of Bone and Joint Surgery - Series A*. https://doi.org/10.2106/00004623-198163090-00012

Bell, A. L., Pedersen, D. R., & Brand, R. A. (1990). A comparison of the accuracy of several hip center location prediction methods. *Journal of Biomechanics*. https://doi.org/10.1016/0021-9290(90)90054-7

Besier, T. F., Sturnieks, D. L., Alderson, J. A., & Lloyd, D. G. (2003). Repeatability of gait data using a functional hip joint centre and a mean helical knee axis. *Journal of Biomechanics*. https://doi.org/10.1016/S0021-9290(03)00087-3

Bessone, V., Höschele, N., Schwirtz, A., & Seiberl, W. (2019). Validation of a new inertial measurement unit system based on different dynamic movements for future in-field applications. *Sports Biomechanics*. https://doi.org/10.1080/14763141.2019.1671486

Bodenheimer, B., Rose, C., Rosenthal, S., & Pella, J. (1997). *The Process of Motion Capture: Dealing with the Data*. https://doi.org/10.1007/978-3-7091-6874-5_1

Cappozzo, A., Catani, F., Della Croce, U., & Leardini, A. (1995). Position and orientation in space of bones during movement: anatomical frame definition and determination. *Clinical Biomechanics*, *10*(4), 171–178. https://doi.org/10.1016/0268-0033(95)91394-T

Carmo, A. A., Kleiner, A. F. R., Lobo da Costa, P. H., & Barros, R. M. L. (2012). Three-dimensional kinematic analysis of upper and lower limb motion during gait of post-stroke patients. *Brazilian Journal of Medical and Biological Research*. https://doi.org/10.1590/S0100-879X2012007500051

Ciğali, B. S., Uluçam, E., & Bozer, C. (2011). 3D motion analysis of hip, knee and ankle joints of children aged between 7-11 years during gait. *Balkan Medical Journal*. https://doi.org/10.5174/tutfd.2010.04199.2

Cuesta-Vargas, A. I., Galán-Mercant, A., & Williams, J. M. (2010). The use of inertial sensors system for human motion analysis. In *Physical Therapy Reviews*. https://doi.org/10.1179/1743288X11Y.0000000006

Cutti, A. G., Ferrari, A., Garofalo, P., Raggi, M., Cappello, A., & Ferrari, A. (2010). "Outwalk": A protocol for clinical gait analysis based on inertial and magnetic sensors. *Medical and Biological Engineering and Computing*. https://doi.org/10.1007/s11517-009-0545-x

Davis, R. B., Õunpuu, S., Tyburski, D., & Gage, J. R. (1991). A gait analysis data collection and reduction technique. *Human Movement Science*. https://doi.org/10.1016/0167-9457(91)90046-Z

El-Zayat, B. F., Efe, T., Heidrich, A., Anetsmann, R., Timmesfeld, N., Fuchs-Winkelmann, S., & Schofer, M. D. (2013). Objective assessment, repeatability, and agreement of shoulder ROM with a 3D gyroscope. *BMC Musculoskeletal Disorders*. https://doi.org/10.1186/1471-2474-14-72

Fernández-Baena, A., Susín, A., & Lligadas, X. (2012). Biomechanical validation of upper-body and lower-body joint movements of kinect motion capture data for

rehabilitation treatments. *Proceedings of the 2012 4th International Conference on Intelligent Networking and Collaborative Systems, INCoS 2012*. https://doi.org/10.1109/iNCoS.2012.66

Ferrari, A., Benedetti, M. G., Pavan, E., Frigo, C., Bettinelli, D., Rabuffetti, M., Crenna, P., & Leardini, A. (2008). Quantitative comparison of five current protocols in gait analysis. *Gait and Posture*. https://doi.org/10.1016/j.gaitpost.2007.11.009

Ferrari, A., Cutti, A. G., Garofalo, P., Raggi, M., Heijboer, M., Cappello, A., & Davalli, A. (2010). First in vivo assessment of "outwalk": A novel protocol for clinical gait analysis based on inertial and magnetic sensors. *Medical and Biological Engineering and Computing*. https://doi.org/10.1007/s11517-009-0544-y

Fong, D. T. P., & Chan, Y. Y. (2010). The use of wearable inertial motion sensors in human lower limb biomechanics studies: A systematic review. In *Sensors (Switzerland)*. https://doi.org/10.3390/s101211556

Fusca, M., Negrini, F., Perego, P., Magoni, L., Molteni, F., & Andreoni, G. (2018). Validation of a wearable IMU system for gait analysis: Protocol and application to a new system. *Applied Sciences (Switzerland)*. https://doi.org/10.3390/app8071167

Gage, J. R. (1990). An overview of normal walking. *Instructional Course Lectures*, *39*, 291–303.

Grieve, D. W., & Gear, R. J. (1966). The relationships between length of stride, step frequency, time of swing and speed of walking for children and adults. *Ergonomics*. https://doi.org/10.1080/00140136608964399

Iwan, W. G. (2006). Principles of Biomechanics and Motion Analysis. *Philadelphia, Williams and Wilkins*, 1–22.

Kharb, A., Saini, V., Jain, Y., & Dhiman, S. (2011). A review of gait cycle and its parameters. *IJCEM Int J Comput Eng Manag*.

Kirtley, C. (2006). *Clinical gait analysis: theory and practice*. Elsevier Health Sciences.

Lythgo, N., Wilson, C., & Galea, M. (2009). Basic gait and symmetry measures for primary school-aged children and young adults whilst walking barefoot and with shoes. *Gait and Posture*. https://doi.org/10.1016/j.gaitpost.2009.07.119

Mancini, M., Chiari, L., Holmstrom, L., Salarian, A., & Horak, F. B. (2016). Validity and reliability of an IMU-based method to detect APAs prior to gait initiation. *Gait and Posture*. https://doi.org/10.1016/j.gaitpost.2015.08.015

Martin Bland, J., & Altman, D. G. (1986). STATISTICAL METHODS FOR ASSESSING AGREEMENT BETWEEN TWO METHODS OF CLINICAL MEASUREMENT. *The Lancet*. https://doi.org/10.1016/S0140-6736(86)90837-8

McGinnis, P. M. (2013). *Biomechanics of sport and exercise*. Human Kinetics.

Norlin, R., Odenrick, P., & Sandlund, B. (1981). Development of gait in the normal child. *Journal of Pediatric Orthopaedics*. https://doi.org/10.1097/01241398-198111000-00004

Nymoen, K. (2014). *Motion Capture*. https://www.uio.no/studier/emner/hf/imv/MUS2006/v15/litteratur/knkap3-4.pdf

Ounpuu, S., Gage, J. R., & Davis, R. B. (1991). Three-dimensional lower extremity joint kinetics in normal pediatric gait. *Journal of Pediatric Orthopaedics*. https://doi.org/10.1097/01241398-199105000-00012

Peck, R., Olsen, C., & Devore, J. L. (2015). *Introduction to statistics and data analysis*. Cengage Learning.

Perry, J., & Burnfield, J. M. (2010). *Gait analysis: normal and pathological function* (2nd ed.). SLACK Incorporated.

Picerno, P., Cereatti, A., & Cappozzo, A. (2008). Joint kinematics estimate using wearable inertial and magnetic sensing modules. *Gait and Posture*. https://doi.org/10.1016/j.gaitpost.2008.04.003

Poitras, I., Dupuis, F., Bielmann, M., Campeau-Lecours, A., Mercier, C., Bouyer, L. J., & Roy, J. S. (2019). Validity and reliability ofwearable sensors for joint angle estimation: A systematic review. In *Sensors (Switzerland)*. https://doi.org/10.3390/s19071555

Robert-Lachaine, X., Mecheri, H., Larue, C., & Plamondon, A. (2017). Validation of inertial measurement units with an optoelectronic system for whole-body motion analysis. *Medical and Biological Engineering and Computing*. https://doi.org/10.1007/s11517-016-1537-2

Robertson, G. E., Caldwell, G. E., Hamill, J., Kamen, G., & Whittlesey, S. (2013). *Research methods in biomechanics*. Human kinetics.

Schiefer, C., Ellegast, R. P., Hermanns, I., Kraus, T., Ochsmann, E., Larue, C., & Plamondon, A. (2014). Optimization of Inertial Sensor-Based Motion Capturing for Magnetically Distorted Field Applications. *Journal of Biomechanical Engineering*. https://doi.org/10.1115/1.4028822

Sharma, A., & Sharma, A. (2013). Motion Capture Process , Techniques and Applications. *Internation Jornal on Recent and Innovation Trends in Computing and Communication*.

Smith, Y., Louw, Q., & Brink, Y. (2016). The three-dimensional kinematics and spatiotemporal parameters of gait in 6-10 year old typically developed children in the Cape Metropole of South Africa - a pilot study. *BMC Pediatrics*. https://doi.org/10.1186/s12887-016-0736-1

Sutherland, D. (1997). The development of mature gait. In *Gait and Posture*. https://doi.org/10.1016/S0966-6362(97)00029-5

Taylor, L., Miller, E., & Kaufman, K. R. (2017). Static and dynamic validation of inertial measurement units. *Gait and Posture*. https://doi.org/10.1016/j.gaitpost.2017.05.026

Todd, F. N., Lamoreux, L. W., Skinner, S. R., Johanson, M. E., St. Helen, R., Moran, S. A., & Ashley, R. K. (1989). Variations in the gait of normal children. A graph applicable to the documentation of abnormalities. *Journal of Bone and Joint Surgery - Series A*. https://doi.org/10.2106/00004623-198971020-00005

van Melick, N., Meddeler, B. M., Hoogeboom, T. J., Nijhuis-van der Sanden, M. W. G., & van Cingel, R. E. H. (2017). How to determine leg dominance: The agreement between self-reported and observed performance in healthy adults. *PLoS ONE*. https://doi.org/10.1371/journal.pone.0189876

Vicon Motion Systems Limited. (2016). *Plug-in Gait Reference Guide*. 95. https://docs.vicon.com/display/Nexus25/PDF+downloads+for+Vicon+Nexus?preview=/50888706/50889377/Plug-in Gait Reference Guide.pdf

Washabaugh, E. P., Kalyanaraman, T., Adamczyk, P. G., Claflin, E. S., & Krishnan, C. (2017). Validity and repeatability of inertial measurement units for measuring gait parameters. *Gait and Posture*. https://doi.org/10.1016/j.gaitpost.2017.04.013

Wheelwright, E. F., Minns, R. A., Law, H. T., & Elton, R. A. (1993). TEMPORAL AND SPATIAL PARAMETERS OF GAIT IN CHILDREN. I: NORMAL CONTROL DATA. *Developmental Medicine & Child Neurology*. https://doi.org/10.1111/j.1469-8749.1993.tb11612.x

Yordanova, S. M., Kostov, N. T., & Kalchev, Y. D. (2016). *Motion Capture Systems Overview and Accelerometer MoCaps Systems*.

Zhang, J.-T., Novak, A. C., Brouwer, B., & Li, Q. (2013). Concurrent validation of Xsens MVN measurement of lower limb joint angular kinematics. *Physiological Measurement*, *34*(8), N63.